N73-17801

NASA CR-121129

THE PREDICTION OF THREE-DIMENSIONAL LIQUID-PROPELLANT ROCKET NOZZLE ADMITTANCES

by

W. A. Bell and B. T. Zinn

GEORGIA INSTITUTE OF TECHNOLOGY

prepared for

NATIONAL AERONAUTICS AND SPACE ADMINISTRATION

NASA Lewis Research Center
Grant NGL 11-002-085
Richard J. Priem, Project Manager

Requests for copies of this report should be referred to:

National Aeronautics and Space Administration
Scientific and Technical Information Facility
P. O. Box 33
College Park, Md. 20740

1. Report No.	2. Government Accession No.	3. Recipient's Catalog No.
NASA CR-121129		

4. Title and Subtitle	5. Report Date
THE PREDICTION OF THREE-DIMENSIONAL LIQUID-PROPELLANT ROCKET NOZZLE ADMITTANCES	February 1973
	6. Performing Organization Code
7. Author(s)	8. Performing Organization Report No.
W. A. Bell and B. T. Zinn	
	10. Work Unit No.
9. Performing Organization Name and Address	
Georgia Institute of Technology Atlanta, Georgia 30332	11. Contract or Grant No. NGL 11-002-085
	13. Type of Report and Period Covered
12. Sponsoring Agency Name and Address	Contractor Report
National Aeronautics and Space Administration Washington, D. C. 20546	14. Sponsoring Agency Code

15. Supplementary Notes

Technical Officer, Richard J. Priem, NASA Lewis Research Center, 21000 Brookpark Road, Cleveland, Ohio 44135

16. Abstract

Crocco's three-dimensional nozzle admittance theory is extended to be applicable when the amplitudes of the combustor and nozzle oscillations increase or decrease with time. An analytical procedure and a computer program for determining nozzle admittance values from the extended theory are presented and used to compute the admittances of a family of liquid-propellant rocket nozzles. The calculated results indicate that the nozzle geometry, entrance Mach number and temporal decay coefficient significantly affect the nozzle admittance values. The theoretical predictions are shown to be in good agreement with available experimental data.

17. Key Words (Suggested by Author(s))	18. Distribution Statement
Combustion instability Liquid rockets Nozzles	Unclassified - unlimited

19. Security Classif. (of this report)	20. Security Classif. (of this page)	21. No. of Pages	22. Price*
Unclassified	Unclassified	55	$3.00

* For sale by the National Technical Information Service, Springfield, Virginia 22151

ABSTRACT

Crocco's three-dimensional nozzle admittance theory is extended to be applicable when the amplitudes of the combustor and nozzle oscillations increase or decrease with time. An analytical procedure and a computer program for determining nozzle admittance values from the extended theory are presented and used to compute the admittances of a family of liquid-propellant rocket nozzles. The calculated results indicate that the nozzle geometry, entrance Mach number and temporal decay coefficient significantly affect the nozzle admittance values. The theoretical predictions are shown to be in good agreement with available experimental data.

TABLE OF CONTENTS

LIST OF ILLUSTRATIONS

LIST OF TABLES

INTRODUCTION

The interaction between the pressure oscillations inside an unstable rocket combustion chamber and the wave motion in the convergent section of the exhaust nozzle can have a significant effect on the stability characteristics of the rocket motor and is an important consideration in analytical studies concerned with the prediction of the stability of liquid-propellant rocket engines. This report is concerned with the investigation of this interaction.

To determine the stability of a liquid-propellant rocket engine, the equations describing the behavior of the oscillatory flow field throughout the rocket motor must be solved. To simplify the problem, it is convenient to analyze the oscillations in the combustion chamber and the nozzle separately. For such an analysis, the combustion chamber extends from the injector face to the nozzle entrance as shown in Fig. 1. All the combustion is assumed to take place in the combustion chamber where the mean flow Mach number is generally assumed to be low. On the other hand, no combustion is assumed to take place in the nozzle and its mean flow Mach number increases from a low value at the nozzle entrance to unity at the throat. Downstream of the throat the flow is supersonic and disturbances in this region cannot propagate upstream and affect the chamber conditions. Therefore, in combustion instability studies it is only necessary to consider the behavior of the oscillations in the converging section of the nozzle since only these oscillations can influence the conditions in the combustion chamber.

The nozzle admittance[1,2] is the boundary condition that must be satisfied by the combustor flow oscillations at the nozzle entrance. Defined as the ratio of the axial velocity perturbation to the pressure perturbation at the nozzle entrance, the nozzle admittance can also be used to determine whether wave motion in the nozzle under consideration adds or removes energy from the combustor oscillations. Furthermore, this boundary condition influences the structures and resonant frequencies of the natural modes of the combustor under investigation.

To theoretically determine the nozzle admittance, the equations which describe the behavior of the waves in the convergent section of the exhaust nozzle must be solved. These equations have been developed by

Crocco[2] and were solved numerically to obtain admittance values for one- and three-dimensional oscillations. These values were tabulated over a wide range of frequencies and entrance Mach numbers for a specific nozzle geometry. By applying the scaling technique developed in Ref. 2, the admittances of related nozzles can be determined. It was pointed out,[2] however, that interpolation of the tabulated values can result in large errors in the predicted nozzle admittances; furthermore, the accuracy of the scaling procedure is open to question. In addition, Crocco's theory is only applicable to constant amplitude periodic wave motions, and in its present form it cannot be applied to cases where the amplitude of the oscillations varies in time.

In this report, the equations needed for computing the nozzle admittance are presented and their solutions are outlined. Crocco's theory is extended to account for wave-amplitude variation with time. Typical theoretical predictions are shown and compared with available experimental data. The effects of the nozzle geometry and chamber Mach number on the nozzle admittance are presented in plots showing frequency dependence of the real and imaginary parts of the nozzle admittance. The effects of the decay coefficient are also assessed. A manual describing the use of the computer program which calculates nozzle admittance values along with a program listing is presented in the appendix.

SYMBOLS

A, B, C	variable coefficients defined below Eq. (14)
c	nondimensional speed of sound, $c^*/\bar{c}_o^*$
$\underset{\sim}{e}_\varphi$, $\underset{\sim}{e}_\psi$, $\underset{\sim}{e}_\theta$	unit vectors
i	$\sqrt{-1}$
J_m	Bessel function of the first kind of order m
$K(\psi,\theta,t)$	a function having the following space and time dependence:

$$J_m\left[S_{mn}\left(\frac{\psi}{\psi_w}\right)^{\frac{1}{2}}\right]e^{i\omega t \pm im\theta}$$

M	Mach number at the nozzle entrance

m	number of mode diametral nodal lines
n	number of mode tangential nodal lines
p	nondimensional pressure, $p^*/\bar{p}^*_o$
q	nondimensional velocity, $\vec{q}^*/\bar{c}^*_o$
r	nondimensional radius, r^*/r^*_c
r_{cc}	nondimensional radius of curvature at the nozzle entrance, r^*_{cc}/r^*_c
r_{ct}	nondimensional radius of curvature at the nozzle throat, r^*_{ct}/r^*_c
S	nondimensional frequency, $\omega^* r^*_c/\bar{c}^*$
S_{mn}	the nth root of the equation $$\frac{dJ_m(x)}{dx} = 0$$
t	nondimensional time, $t^*\bar{c}^*_o/r^*_o$
u	nondimensional axial velocity component, $u^*/\bar{c}^*_o$
v	nondimensional radial velocity component, $v^*/\bar{c}^*_o$
w	nondimensional tangential velocity component, $w^*/\bar{c}^*_o$
y	irrotational specific nozzle admittance defined in Eq. (13) $$y = \bar{\rho}^*\bar{c}^* \frac{u'^*}{p'^*} = \gamma\bar{\rho}\bar{c}\, \frac{u'}{p'}$$
z	nondimensional axial coordinate, z^*/r^*_c
γ	ratio of specific heats
ζ	a function used to compute the nozzle admittance; defined below Eq. (13)
θ	tangential coordinate, radians
θ_1	nozzle half-angle, degrees
λ	nondimensional temporal decay coefficient, $\lambda^* r^*_c/\bar{c}^*_o$
ρ	nondimensional density, $\rho^*/\bar{\rho}^*_o$
τ	a function used to compute the nozzle admittance; $\tau = 1/\zeta$
φ	nondimensional steady state velocity potential, $\varphi^*/\bar{c}^*_o r^*_c$
Φ	a function describing the φ-dependence of the radial velocity perturbation
ψ	nondimensional steady state stream function, $\frac{1}{2}\bar{\rho}(\varphi)\,\bar{q}(\varphi)\,r^2$
ω	nondimensional frequency, $\omega^* r^*_c/\bar{c}^*_o$

Subscripts:

c	evaluated at the chamber wall
i	imaginary part of a complex quantity
o	stagnation value
r	real part of a complex quantity
th	evaluated at the nozzle throat
w	evaluated at the nozzle wall
$\rightarrow$	vector quantity

Superscripts:

$'$	perturbation quantity
$-$	steady state value
$*$	dimensional quantity

ANALYSIS

Derivation of the Wave Equations

The equations used by Crocco[2] to compute the nozzle admittance will be developed from the conservation equations. To keep the problem mathematically tractable and yet physically meaningful, the following assumptions were employed.

(1) The nozzle flow is a calorically perfect gas consisting of a single species.

(2) Viscosity and heat conduction are negligible.

(3) The steady state flow is one-dimensional; this assumption implies that the nozzle is slowly converging.

(4) The amplitudes of the waves are small so that only linear terms in the perturbed quantities need to be retained in the conservation equations.

(5) The oscillations are assumed to be irrotational.

Using these assumptions, the equations of motion in nondimensional form become

Continuity

$$\frac{\partial \rho}{\partial t} + \nabla \cdot (\rho q) = 0 \tag{1}$$

Momentum

$$\frac{\partial \underset{\rightarrow}{q}}{\partial t} + \tfrac{1}{2}\nabla \bar{q}^2 = -\frac{1}{\rho}\nabla p \tag{2}$$

and, from the isentropic conditions, $c^2 = p/\rho$ and $p = \rho^\gamma$.

To obtain the linearized wave equations, the dependent variables are expressed in the following form:

$$\underset{\rightarrow}{q} = \bar{q} + q', \quad p = \bar{p} + p', \quad \rho = \bar{\rho} + \rho' \tag{3}$$

Substituting these expressions into Eqs. (1) and (2), neglecting all non-linear terms involving primed quantities, and separating the resulting system of equations into a set of steady state equations and a set of unsteady equations yield the system of steady state equations:

$$\nabla\cdot(\bar{\rho}\underset{\rightarrow}{\bar{q}}) = 0; \quad \bar{c}^2 = \bar{\rho}^{\gamma - 1} = 1 - \frac{\gamma - 1}{2}\bar{q}^2; \quad \bar{p} = \bar{\rho}^\gamma \tag{4}$$

and the following system of unsteady linear equations that describe the wave motion:

$$\frac{\partial \rho'}{\partial t} + \nabla\cdot(\underset{\rightarrow}{\bar{q}}\rho' + \bar{\rho}\underset{\rightarrow}{q'}) = 0 \tag{5}$$

$$\frac{\partial \underset{\rightarrow}{q'}}{\partial t} + \nabla(\bar{q}\cdot q') = -\nabla\left(\frac{p'}{\gamma\bar{\rho}}\right) \tag{6}$$

$$p' = \bar{c}^2\rho' \tag{7}$$

To simplify the application of the boundary conditions at the nozzle walls, these wave equations are solved in the orthogonal coordinate system shown in Fig. 1. In this coordinate system the steady state velocity potential φ replaces the axial coordinate z, the steady state stream function ψ replaces the radial coordinate r and the angle θ is used to denote azimuthal variations. Using this coordinate system the velocity vectors can be expressed as follows:

$$\underset{\rightarrow}{\bar{q}} = \bar{q}(\varphi)\,\underset{\rightarrow}{e}_{\varphi}$$

$$\underset{\rightarrow}{q}' = u'\underset{\rightarrow}{e}_{\varphi} + v'\underset{\rightarrow}{e}_{\psi} + w'\underset{\rightarrow}{e}_{\theta}$$

Using the definitions of the steady state velocity potential and stream function for a one-dimensional mean flow, it can be shown[2] that

$$q(\varphi) = \frac{d\varphi}{dz}$$

$$\psi = \tfrac{1}{2}\bar{\rho}(\varphi)\,\bar{q}(\varphi)\,r^2$$

Rewriting Eqs. (5) and (6) in the (φ,ψ,θ) coordinate system yields the following system of equations[2]:

Continuity

$$\frac{\partial}{\partial t}\left(\frac{\rho'}{\bar{\rho}}\right) + \bar{q}^2\,\frac{\partial}{\partial\varphi}\left(\frac{\rho'}{\bar{\rho}} + \frac{u'}{\bar{q}}\right) + 2\bar{\rho}\bar{q}\,\frac{\partial}{\partial\psi}\left(\frac{v'}{r\bar{\rho}\bar{q}}\right) + \frac{\bar{\rho}\bar{q}}{2\psi}\,\frac{\partial(rw')}{\partial\theta} = 0 \tag{8}$$

Momentum

φ-component

$$\frac{\partial\left(\frac{u'}{\bar{q}}\right)}{\partial t} + \frac{\partial}{\partial\varphi}\left(\bar{q}^2\,\frac{u'}{\bar{q}}\right) + \frac{\partial}{\partial\varphi}\left(\frac{p'}{\gamma\bar{p}}\right) = 0 \tag{9}$$

ψ-component

$$\frac{\partial}{\partial t}\left(\frac{v'}{r\bar{\rho}\bar{q}}\right) + \bar{q}^2\,\frac{\partial}{\partial\varphi}\left(\frac{v'}{r\bar{\rho}\bar{q}}\right) + \frac{\partial}{\partial\psi}\left(\frac{p'}{\gamma\bar{p}}\right) = 0 \tag{10}$$

θ-component

$$\frac{\partial}{\partial t}(rw') + \bar{q}^2\,\frac{\partial}{\partial\varphi}(rw') + \frac{\partial}{\partial\theta}\left(\frac{p'}{\gamma\bar{p}}\right) = 0 \tag{11}$$

Equations (7) through (11) constitute a system of five equations in the five unknowns -- $\rho'/\bar{\rho}$, $u'/\bar{q}$, $v'/r\bar{\rho}\bar{q}$, rw', and $p'/\gamma\bar{p}$. These equations are solved by the method of separation of variables and the solutions are

$$\frac{u'}{\bar{q}} = \frac{d\Phi(\varphi)}{d\varphi} K(\psi,\theta,t)$$

$$\frac{v'}{r\bar{\rho}\bar{q}} = \Phi(\varphi) \frac{\partial}{\partial\psi}\left[K(\psi,\theta,t)\right]$$

$$rw' = \Phi(\varphi) \frac{\partial}{\partial\theta}\left[K(\psi,\theta,t)\right]$$

$$\frac{p'}{\bar{p}} = -\left[i(\omega - i\lambda)\Phi(\varphi) + \bar{q}^2(\varphi) \frac{d\Phi(\varphi)}{d\varphi}\right] K(\psi,\theta,t)$$

$$\frac{\rho'}{\bar{\rho}} = -\frac{1}{\bar{c}^2}\left[i(\omega - i\lambda)\ \Phi(\varphi) + \bar{q}^2(\varphi) \frac{d\Phi(\varphi)}{d\varphi}\right] K(\psi,\theta,t)$$

where

$$K(\psi,\theta,t) = \begin{cases} J_m\left[S_{mn}\left(\frac{\psi}{\psi_w}\right)^{\frac{1}{2}}\right] \cos m\theta\, e^{i(\omega - i\lambda)t} & \textit{for standing waves} \\ J_m\left[S_{mn}\left(\frac{\psi}{\psi_w}\right)^{\frac{1}{2}}\right] e^{\pm im\theta}\ e^{i(\omega - i\lambda)t} & \textit{for spinning waves} \end{cases}$$

These solutions identically satisfy the momentum and energy equations. Substituting these solutions into Eq. (8) and eliminating variables give the following differential equation for the function Φ:

$$\bar{q}^2(\bar{c}^2 - \bar{q}^2)\frac{d^2\Phi}{d\varphi^2} - \bar{q}^2\left[\frac{1}{\bar{c}^2}\frac{d\bar{q}^2}{d\varphi} + 2i(\omega - i\lambda)\right]\frac{d\Phi}{d\varphi}$$
$$+ \left[(\omega - i\lambda)^2 - \frac{\gamma - 1}{2}\, i(\omega - i\lambda)\frac{\bar{q}^2}{\bar{c}^2}\frac{d\bar{q}^2}{d\varphi} - \frac{S_{mn}^2\bar{c}^2}{r_w^2}\right]\Phi = 0 \tag{12}$$

The function Φ can be related to the specific acoustic admittance by the formula[2]

$$y = \gamma\bar{p}\bar{c}\,\frac{u'}{p'} = -\frac{\gamma\bar{p}\bar{c}\zeta}{\bar{q}^2\zeta + i(\omega - i\lambda)} \tag{13}$$

where $\zeta = \frac{1}{\Phi}\frac{d\Phi}{d\varphi}$. Using the definition of ζ and Eq. (12), the following differential equation for ζ is derived:

$$\frac{d\zeta}{d\varphi} - \frac{B}{A}\zeta + \zeta^2 = -\frac{C}{A} \tag{14}$$

where

$$A = \bar{q}^2(\bar{c}^2 - \bar{q}^2)$$

$$B = \bar{q}^2\left[\frac{1}{\bar{c}^2}\frac{d\bar{q}^2}{d\varphi} + 2i(\omega - i\lambda)\right]$$

$$C = \left[(\omega - i\lambda)^2 - \frac{S_{mn}^2\bar{c}^2}{r_w^2} - i(\omega - i\lambda)\frac{\gamma - 1}{2}\frac{\bar{q}^2}{\bar{c}^2}\frac{d\bar{q}^2}{d\varphi}\right]$$

Equation (14) is a complex Riccati equation which must be solved numerically to obtain ζ. Once the value of ζ is determined at the nozzle entrance, the nozzle admittance can be computed directly from Eq. (13). Inspection of Eq. (14) shows that the value of ζ depends upon its coefficients A, B, and C which in turn depend upon ω, λ, S_{mn}, and the space dependence of $\bar{q}$ and $\bar{c}$ in the nozzle. The behavior of $\bar{q}$ and $\bar{c}$ in the nozzle can be computed once the value of γ and the nozzle contour are specified.

To determine ζ for given values of ω, λ, S_{mn} and γ and a specific nozzle contour, Eq. (14) must be integrated numerically. A major difficulty which can occur during this integration is that ζ becomes unbounded whenever Φ approaches zero, which causes numerical difficulties in the integration scheme. Crocco and Sirignano[2] noted that this phenomenon occurred for low Mach numbers and high values of ω/S_{mn}. At these Mach numbers and frequencies they developed asymptotic solutions for ζ.

Instead of using the asymptotic solution, an exact numerical solution is obtained in this study. The problem is resolved by introducing a new dependent variable

$$\tau = \frac{1}{\zeta} = \frac{\Phi}{\frac{d\Phi}{d\varphi}}$$

As Φ approaches zero and the magnitude of ζ becomes large, τ becomes small. Introducing the definition of τ into Eq. (14) gives the following Riccati equation for τ

$$\frac{d\tau}{d\varphi} + \frac{B}{A}\tau - \frac{C}{A}\tau^2 = 1 \tag{15}$$

At those regions where ζ becomes unbounded, Eq. (15) is integrated instead of Eq. (14).

Method of Solution

To obtain the nozzle admittance from Eq. (13), values of ζ and τ are computed by numerically integrating Eq. (14) or (15). To evaluate the coefficients A, B, and C, a differential equation that describes the variations of the steady state velocity in the subsonic portion of the nozzle must be derived. Differentiating the continuity equation

$$\bar{\rho} r^2 \bar{q} = \bar{\rho}_{th}\, r_{th}^2\, \bar{q}_{th} = \text{constant} \tag{16}$$

where $\bar{q}_{th}^2 = \bar{c}_{th}^2 = 2/(\gamma + 1)$, and using Eq. (4) yield the following differential equation

$$\frac{d\bar{q}^2}{dr} = \frac{1}{dr/d\bar{q}^2} = -\frac{4}{r_{th}}\left(\frac{2}{\gamma + 1}\right)^{\frac{-\gamma - 1}{4(\gamma - 1)}}\left[\frac{(\bar{q}^2)^{\frac{5}{4}}\left(1 - \frac{\gamma - 1}{2}\bar{q}^2\right)^{\frac{2\gamma - 1}{2(\gamma - 1)}}}{1 - \frac{\gamma + 1}{2}\bar{q}^2}\right] \tag{17}$$

Using Eq. (17) and the specified nozzle contour in terms of $r(z)$, the quantity $d\bar{q}/d\varphi$ can be obtained from the relationship

$$\frac{d\bar{q}^2}{d\varphi} = \frac{d\bar{q}^2}{dr}\frac{dr}{dz}\frac{dz}{d\varphi} = 2\,\frac{d\bar{q}}{dr}\frac{dr}{dz} \tag{18}$$

Once $\bar{q}^2$ is known the corresponding value of $\bar{c}^2(\varphi)$ can be obtained by use of Eq. (4). To evaluate dr/dz in Eq. (18), the nozzle contour shown in Fig. 2 is used. Starting at the combustion chamber the contour is generated by a circular arc of radius r_{cc} turned through an angle θ_1, the nozzle half-angle. This arc connects smoothly to a straight line which is inclined at an angle θ_1 to the nozzle axis. This straight line then joins with another circular arc of radius r_{ct} which turns through an angle θ_1 and ends at the throat. Using this nozzle contour, in regions I, II and III of Fig. 2

$$\left.\frac{dr}{dz}\right|_{I} = - \frac{\left[2r_{ct}(r - r_{th}) - (r - r_{th})^2\right]^{\frac{1}{2}}}{r_{ct} + r_{th} - r}$$

$$\left.\frac{dr}{dz}\right|_{II} = - \tan \theta_1$$

$$\left.\frac{dr}{dz}\right|_{III} = \frac{\left[2r_{cc}(1 - r) - (1 - r)^2\right]^{\frac{1}{2}}}{1 - r_{cc} - r}$$

Utilizing the appropriate expression for dr/dz, Eq. (18) can now be solved simultaneously with Eq. (14) or (15) to determine the nozzle admittance.

The numerical integration of these equations must start at some initial point where the initial conditions are known. Since the equation for ζ is singular at the throat[2], the integration is initiated at a point that is located a short distance upstream of the throat. The needed initial conditions are obtained by expanding the dependent variables in a Taylor series about the throat. To obtain this Taylor series, its coefficients $\zeta(0) = \zeta_0$ and $\zeta_1 = \left.\frac{d\zeta}{d\varphi}\right|_{\varphi = 0}$ must be evaluated at the throat where $\varphi = 0$. These coefficients are evaluated by substituting the series

$$\zeta = \zeta_0 + \zeta_1\varphi + \ldots$$

into Eq. (14) and taking the limit as $\varphi \to 0$. The results are

$$\zeta_0 = \zeta(0) = \frac{C_0}{B_0}$$

$$\zeta_1 = \left.\frac{d\zeta}{d\varphi}\right|_{\varphi = 0} = \left[B_1\left(\frac{C_0}{B_0}\right) - A_1\left(\frac{C_0}{B_0}\right)^2 - C_1\right]/(A_1 - B_0)$$

where

$$C_0 = C\Big|_{\varphi = 0} = \left[(\omega - i\lambda)^2 - i\,\frac{2(\gamma - 1)(\omega - i\lambda)}{(\gamma + 1)\sqrt{r_{th} r_{ct}}} - \frac{S_{mn}^{\;2}}{r_{th}^{\;2}}\left(\frac{2}{\gamma + 1}\right)\right]$$

$$B_0 = B\Big|_{\varphi = 0} = \frac{4}{\gamma + 1}\left[\frac{1}{\sqrt{r_{th} r_{ct}}} + i(\omega - i\lambda)\right]$$

$$B_1 = \frac{dB}{d\varphi}\Big|_{\varphi = 0} = \frac{4}{\gamma + 1}\left[\frac{6 + \gamma}{3 r_{th} r_{ct}} + i\,\frac{2(\omega - i\lambda)}{\sqrt{r_{th} r_{ct}}}\right]$$

$$A_1 = \frac{dA}{d\varphi}\Big|_{\varphi = 0} = \frac{-4}{(\gamma + 1)\sqrt{r_{th} r_{ct}}}$$

$$C_1 = \frac{dC}{d\varphi}\Big|_{\varphi = 0} = 2\left(\frac{\gamma - 1}{\gamma + 1}\right)\left[\frac{S_{mn}^{\;2}}{r_{th}^{\;2}\sqrt{r_{th} r_{ct}}} - \frac{i(\omega - i\lambda)}{3 r_{th} r_{ct}}(6 + \gamma)\right]$$

The following relations are used in the evaluation of the above quantities:

$$\bar{q}^2\Big|_{\varphi = 0} = \frac{2}{\gamma + 1}$$

$$\frac{d\bar{q}^2}{d\varphi}\Big|_{\varphi = 0} = \frac{4}{(\gamma + 1)\sqrt{r_{th} r_{ct}}}$$

Once ζ_0 and ζ_1 are known, the initial condition at $\varphi = \varphi_1$ is obtained from the expression $\zeta(\varphi_1) = \zeta_0 + \zeta_1 \varphi_1$.

The numerical solution is obtained by use of a modified Adams predictor-corrector scheme, and employing a Runge-Kutte scheme of order four to start the numerical integration. Initially, Eqs. (14) and (18) are integrated to determine ζ; if the magnitude of ζ exceeds a specified value at which numerical difficulties can occur, the integration of Eq. (14) is terminated. Using the value of ζ at that point, τ is computed and the integration proceeds using Eq. (15). Similarly, should the magnitude of τ become excessively large, the integration of Eq. (15) is terminated, ζ is computed from the value of τ at that point, and the integration proceeds using Eq. (14). This process is repeated until the nozzle entrance is reached. A computer program utilizing this procedure has been written in FORTRAN V for use on the UNIVAC 1108 computer and it is presented in the Appendix.

RESULTS AND DISCUSSION

Using the previously mentioned computer program, theoretical values of the real and imaginary parts of the nozzle admittance have been computed for several nozzle configurations having contours similar to the one presented in Fig. 2. In these computations the radii of curvature, r_{cc} and r_{ct}, are assumed to be equal. The admittance values are presented as functions of the nondimensional frequency S in Figs. 3 through 9 where they are compared with available experimental data obtained from Ref. 3. In these figures, the frequency has been nondimensionalized by the ratio of the steady state speed of sound at the nozzle entrance to the chamber radius r_c.

Admittances for Longitudinal Modes

Longitudinal-type instabilities in general occur in the range of S from 0 to approximately 1.8 which is in the vicinity of the cutoff frequency of the first tangential modes. The cutoff frequency of a particular transverse mode is $S_{mn}\sqrt{(1 - M^2)}$ where S_{mn} is the transverse mode eigenvalue and the subscripts m and n respectively denote the number of diametral nodal lines and the number of tangential nodal lines. Values of S_{mn} are given in Table 1 for several values of m and n.

For longitudinal modes good agreement exists between the experimental and theoretical values of the real and imaginary parts of the admittance as shown in Figs. 3 through 5. The effect of changing the nozzle half-angle is presented in Fig. 3 for a nozzle with an entrance Mach number M of 0.08 and $r_{cc}/r_c = 0.44$. The data indicate that increasing θ_1 increases the frequency at which the real and imaginary parts of the admittance attain maximum values. These data also indicate that the assumption of a one-dimensional mean flow

Table 1. Values of Transverse Mode Eigenvalues; S_{mn}

Transverse Wave Pattern	m	n	S_{mn}
Longitudinal	0	0	0
First Tangential (1T)	1	0	1.8413
Second Tangential (2T)	2	0	3.0543
First Radial (1R)	0	1	3.8317
Third Tangential (3T)	3	0	4.2012
Fourth Tangential (4T)	4	0	5.3175
First Tangential, First Radial (1T,1R)	1	1	5.3313
Fifth Tangential (5T)	5	0	6.4154
Second Tangential, First Radial (2T,1R)	2	1	6.7060
Second Radial (2R)	0	2	7.0156

used in the development of the theory appears to be valid. Even for nozzles with half-angles as high as 45 degrees, for which it has been shown that the mean flow is two-dimensional,[4] the experimental and theoretical nozzle admittance values are in good agreement.

Examination of Fig. 4 shows that the entrance Mach number M has a significant effect on the admittance values for $\theta_1 = 15$ degrees and $r_{cc}/r_c = 0.44$. However, increasing the nozzle half-angle appears to decrease the influence of the entrance Mach number, and for $\theta_1 = 45$ degrees variations in M has little effect.[3] The dependence of the nozzle admittance upon the radius of curvature for a nozzle with $M = 0.16$ and $\theta_1 = 30$ degrees is shown in Fig. 5.

The data presented in Figs. 3 through 5 show that for longitudinal modes the real part of the nozzle admittance is always positive. As indicated by Crocco[1,2] positive values of the real part of the nozzle admittance imply that the nozzle removes acoustic energy from the combustor wave system which implies that the nozzle exerts a stabilizing influence upon the chamber oscillations.

In combustion instability analyses of liquid-propellant rocket motors, it is often assumed that the nozzle is short. This assumption implies that the nozzle length and throat diameter are much smaller than the chamber length and diameter so that the wave travel time in the nozzle is much shorter than the wave travel time in the chamber. For a short nozzle the real and imaginary parts of the admittance are independent of frequency and are given by the expressions[5]

$$y_r = \frac{\gamma - 1}{2} M \; ; \qquad y_i = 0$$

These theoretical short nozzle admittance results do not agree with the results obtained for typical liquid rocket nozzles presented in Figs. 3 through 5. The disagreement is especially evident for nozzles with low values of θ_1, which imply that the nozzle is long, and for high values of S where the wave length of the oscillation becomes of the same order of magnitude as a characteristic nozzle dimension.

Admittances for Mixed First Tangential-Longitudinal Modes

The mixed first tangential-longitudinal modes are those three-dimensional modes which exist between the cutoff frequencies of the first tangential ($S \simeq 1.8$) and second tangential ($S \simeq 3.0$) modes. Theoretical and experimental nozzle admittance data for these modes are presented in Figs. 6 through 8.

In Fig. 6 the influence of the nozzle half-angle on the admittance values is shown. The theoretical and experimental results are in good agreement and they indicate that increasing θ_1 increases the frequency at which the real and imaginary parts of the admittance reach maximum values.

The effect of Mach number on the admittance values is presented in Fig. 7 for $\theta_1 = 15$ degrees and $r_{cc}/r_c = 0.44$. Mach number effects are especially significant at the higher frequencies. However, as shown in Ref. 3, increasing the nozzle half-angle decreases the dependence of the admittance values on the Mach number. The effect of changing the radii of curvature on the admittance values is presented in Fig. 8.

The results presented in Figs. 6 through 8 show that for mixed first tangential-longitudinal modes the real part of the nozzle admittance can be negative which means that the nozzle radiates wave energy back into the combustor; this process exerts a destabilizing influence on the oscillations in the chamber.[2] These negative values occur only for three-dimensional modes and, as shown by Crocco,[2] their cause can be traced to the term involving S_{mn} in Eq. (12). For longitudinal modes, for which S_{mn}

is zero, the real part of the nozzle admittance is always positive, and for those modes the nozzle always exerts a stabilizing influence upon the combustor oscillations.

Effect of Decay Coefficient upon Admittance Data

The nozzle admittance theory has been modified to include the effects of a temporal decay coefficient, λ. Typical results are shown in Figs. 9 and 10 for values of λ of -0.05, 0, and 0.05. These results indicate that varying λ affects both the real and imaginary parts of the admittance. Therefore, the decay coefficient should be included in the nozzle admittance computations when the oscillations are not neutrally stable.

SUMMARY AND CONCLUSIONS

The equations necessary to determine the nozzle admittance for one- and three-dimensional oscillations have been developed. The analytical approach used in solving the nozzle wave equations is outlined and employed to obtain nozzle admittance data for typical nozzle configurations. These data show the dependence of the nozzle admittance values upon nozzle geometry, nozzle Mach number, mode of oscillation, and the temporal damping coefficient.

The results can be summarized as follows for longitudinal and mixed first tangential-longitudinal modes. Decreasing the nozzle length by increasing the nozzle half-angle and Mach number or by decreasing the throat and entrance radii of curvature decreases the frequency dependence of the nozzle admittance. Good agreement exists between the theoretical predictions and available experimental data. However, the nozzle admittance values for typical liquid rocket nozzles are not in agreement with the values obtained from short nozzle theory. Including the effects of a temporal damping coefficient in the nozzle admittance computations changes the admittance values. Therefore, when the oscillations are not neutrally stable, the temporal decay coefficient should be accounted for in the computations.

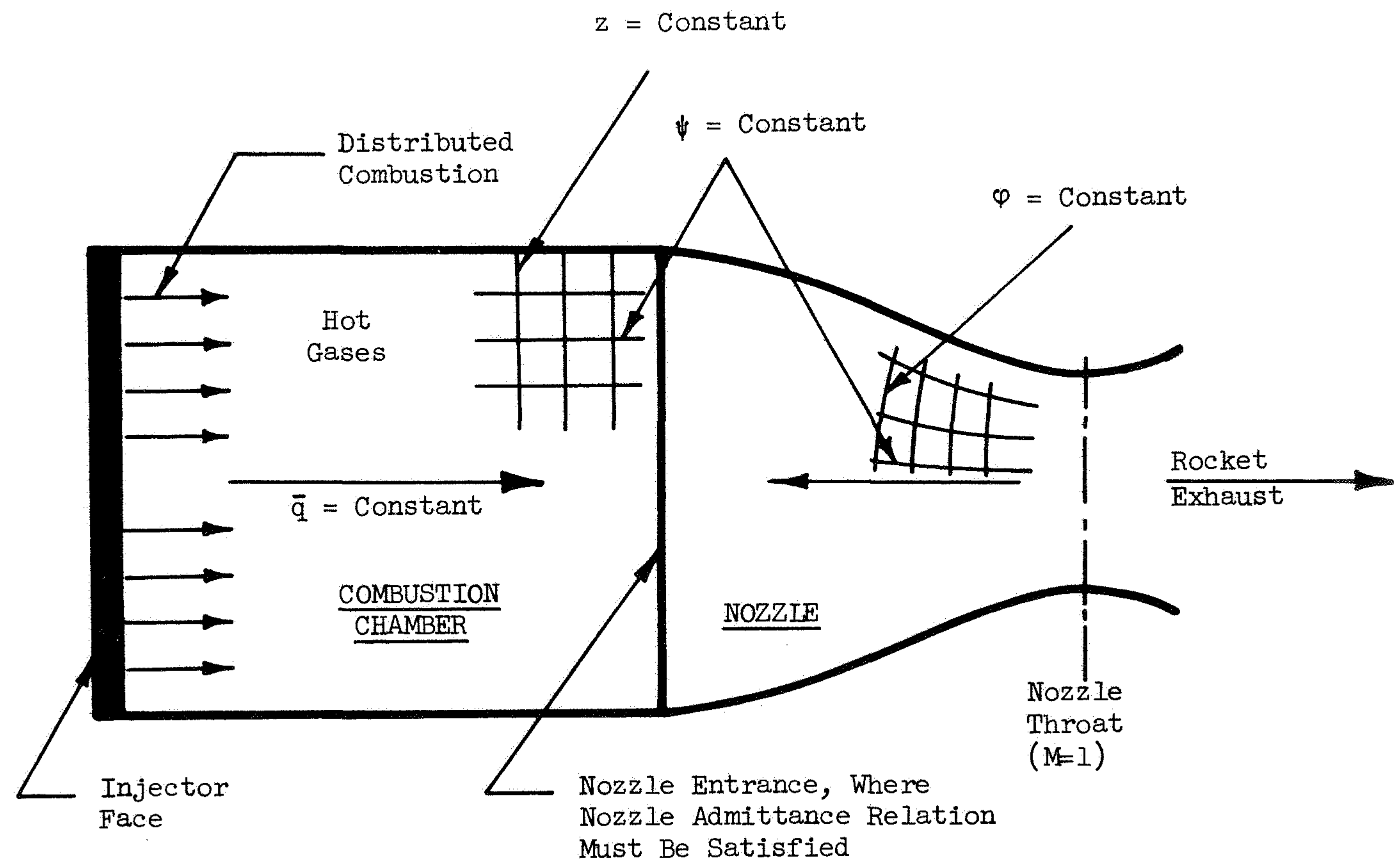

Figure 1. Typical Mathematical Model of a Liquid Rocket Engine

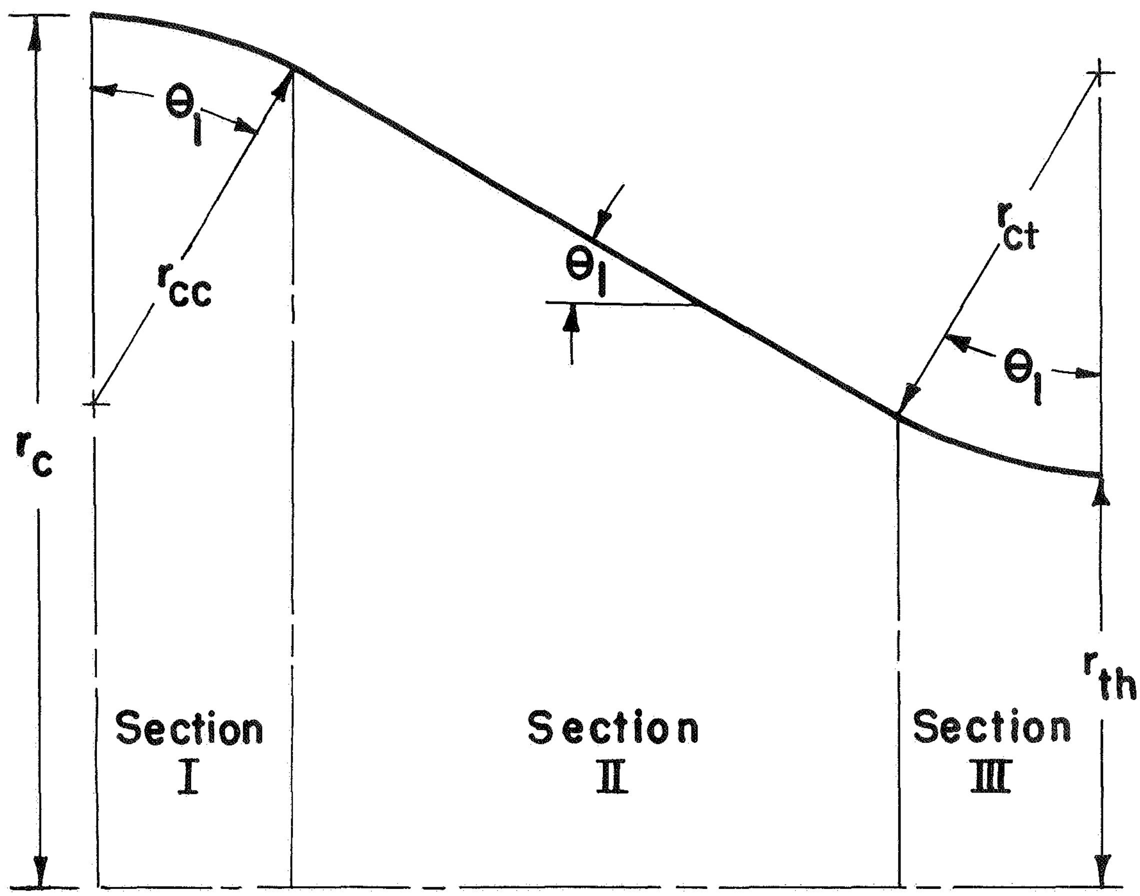

Figure 2. Nozzle Contour

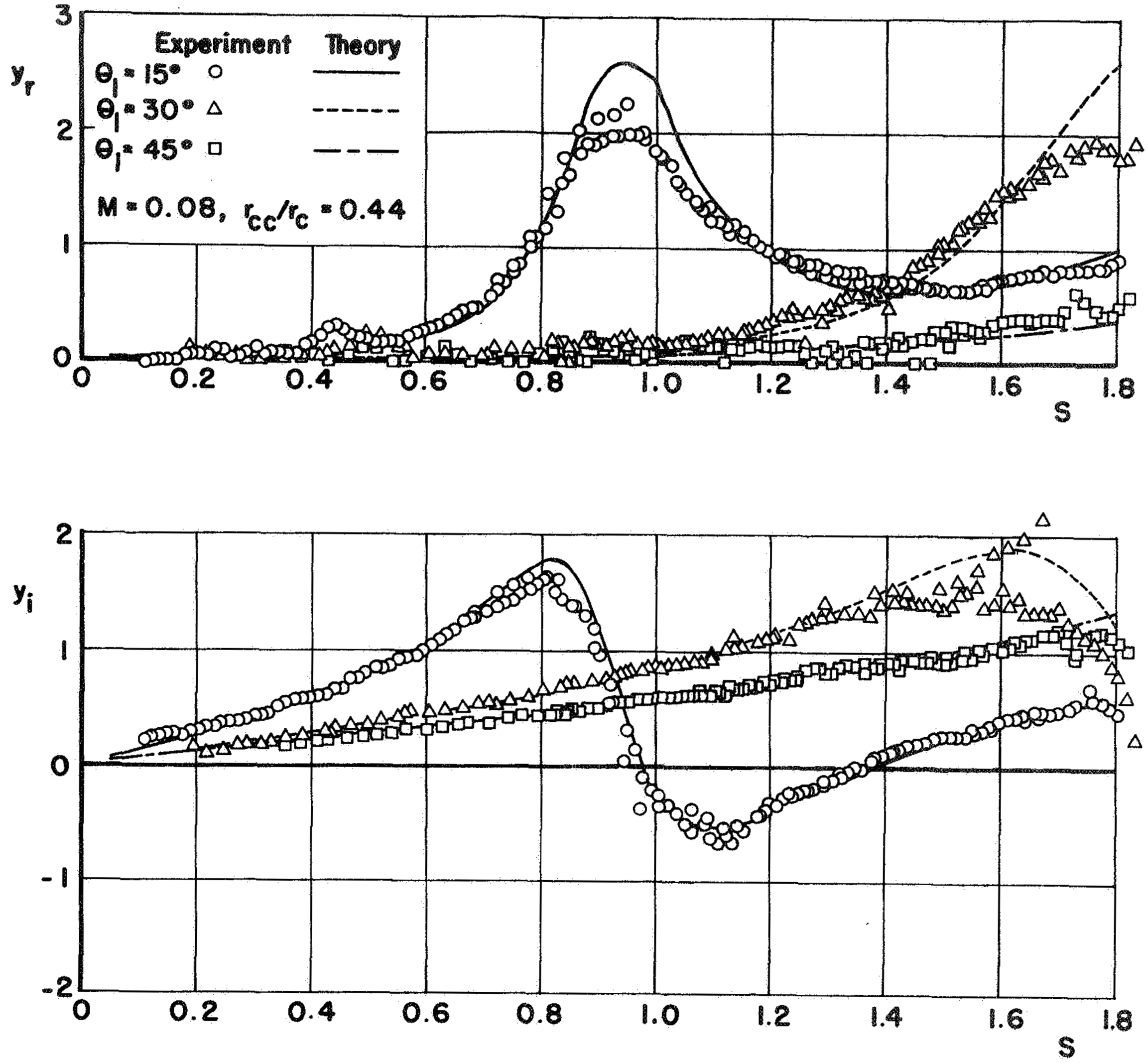

Figure 3. The Effect of Nozzle Half-Angle on the Theoretical and Experimental Nozzle Admittance Values for Longitudinal Modes

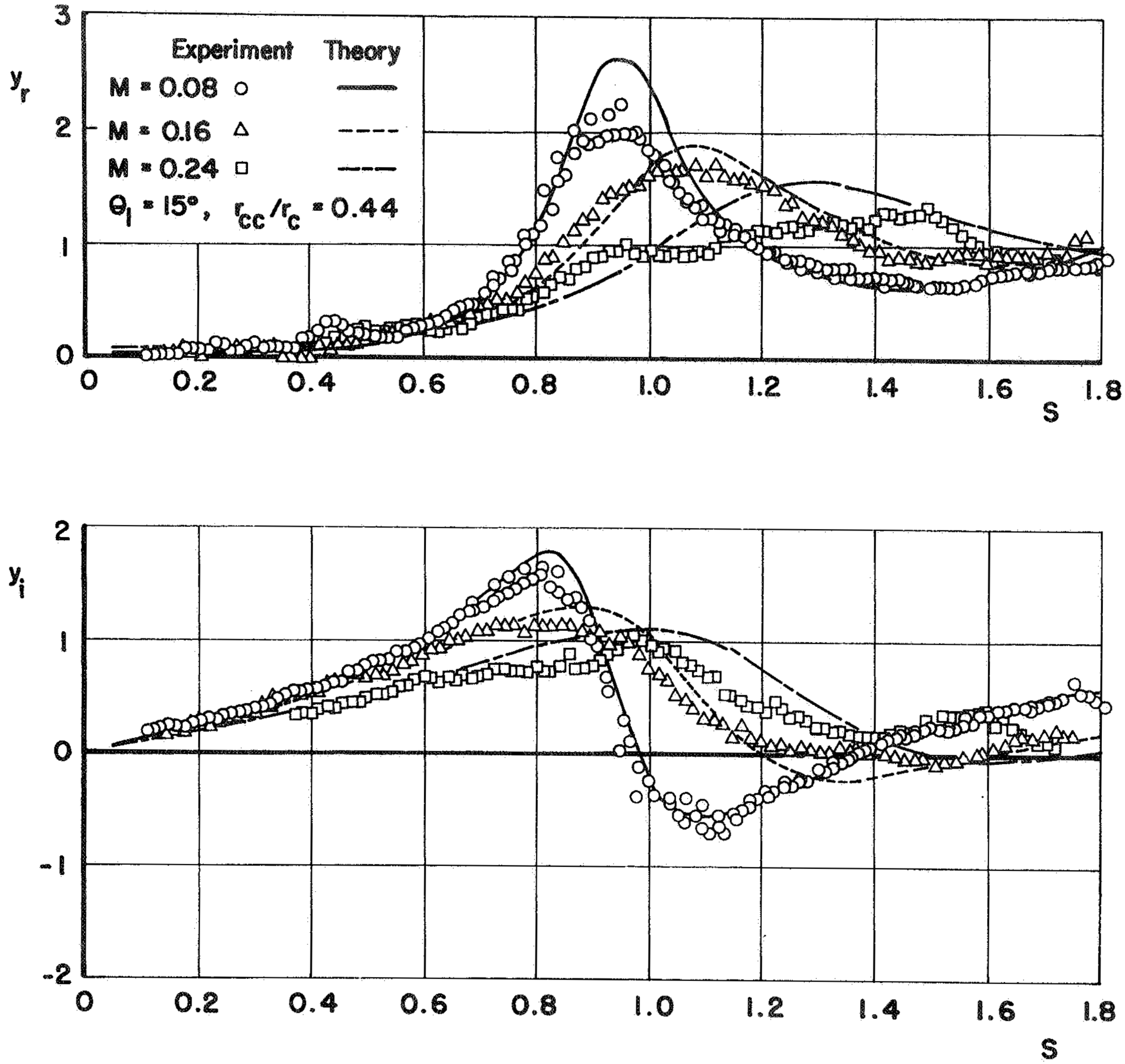

Figure 4. The Effect of Entrance Mach Number on the Theoretical and Experimental Nozzle Admittance Values for Longitudinal Modes

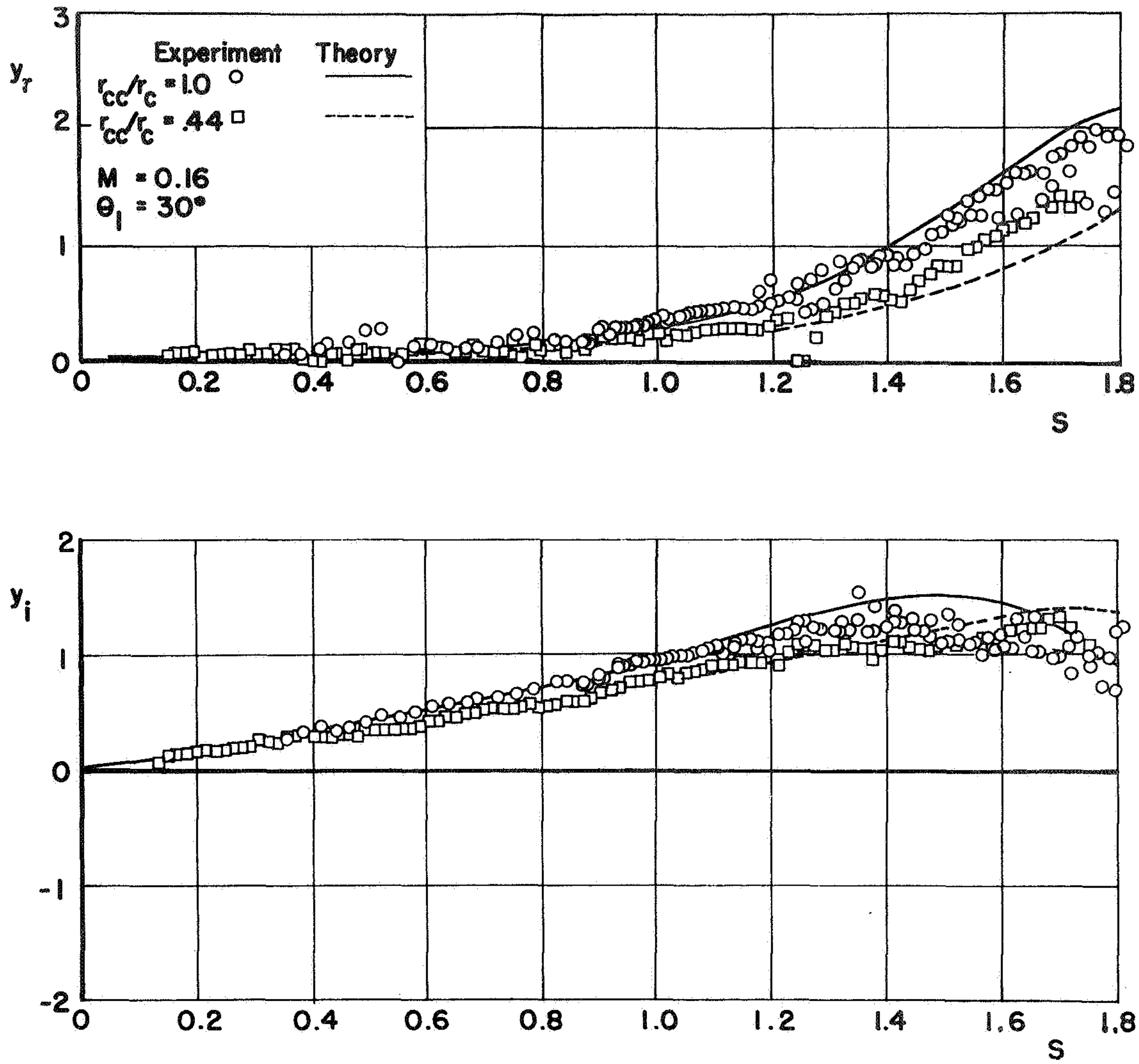

Figure 5. The Effect of the Radii of Curvature on the Theoretical and Experimental Nozzle Admittance Values for Longitudinal Modes

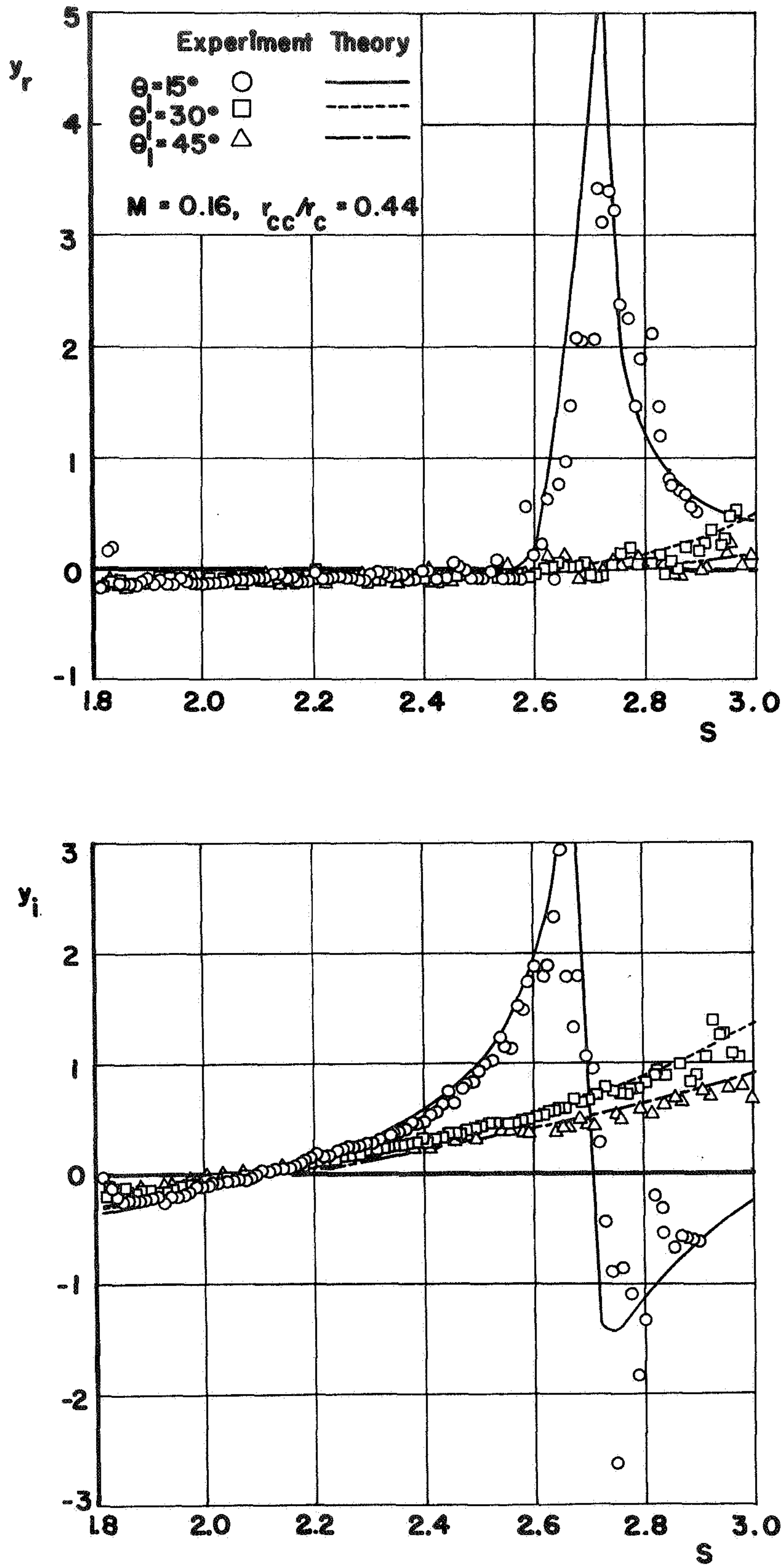

Figure 6. The Effect of the Nozzle Half-Angle on the Theoretical and Experimental Nozzle Admittance Values for Mixed First Tangential-Longitudinal Modes

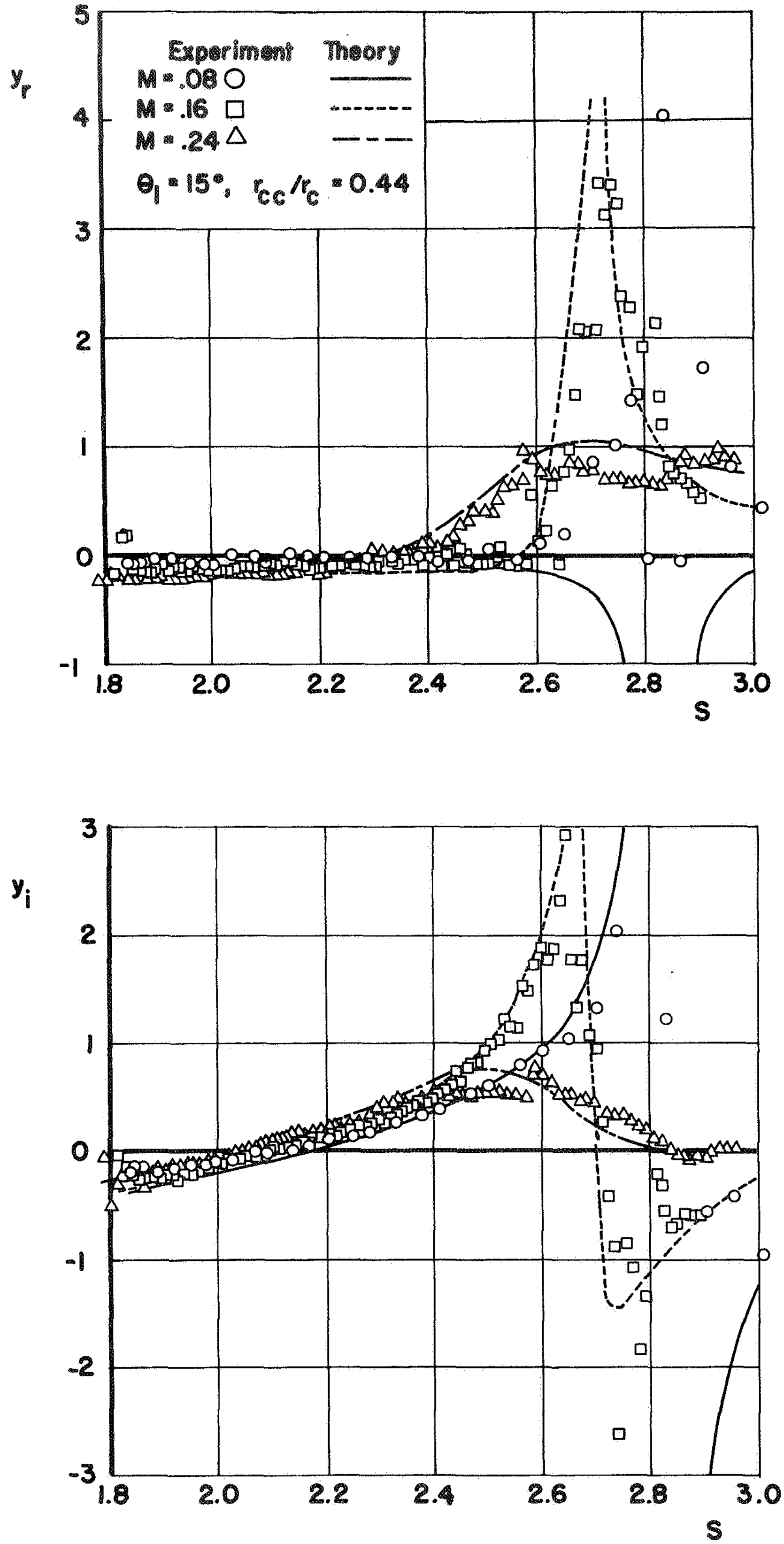

Figure 7. The Effect of Entrance Mach Number on the Theoretical and Experimental Nozzle Admittance Values for Mixed First Tangential-Longitudinal Modes

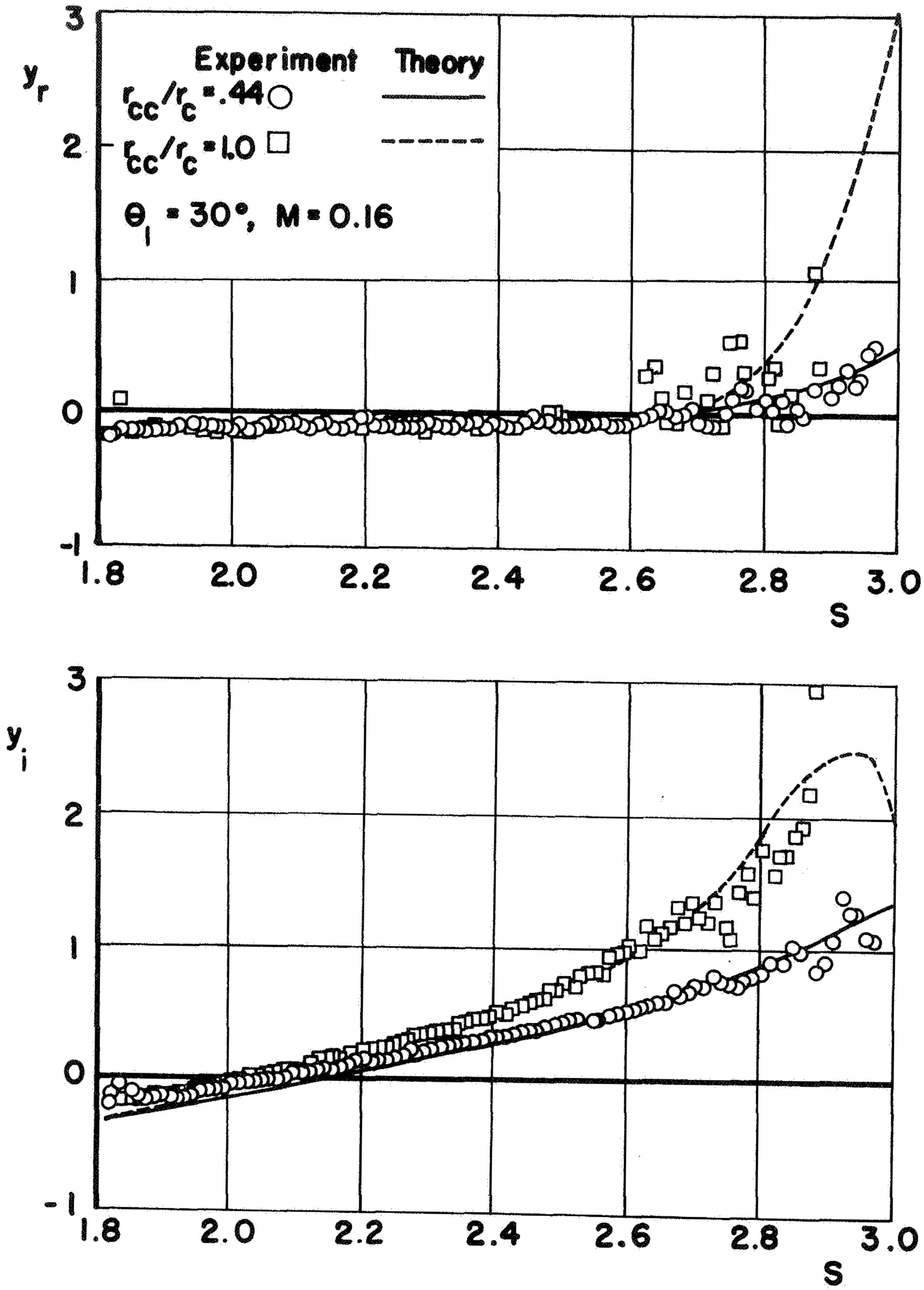

Figure 8. The Effect of the Radii of Curvature on the Theoretical and Experimental Nozzle Admittance Values for Mixed First Tangential-Longitudinal Modes

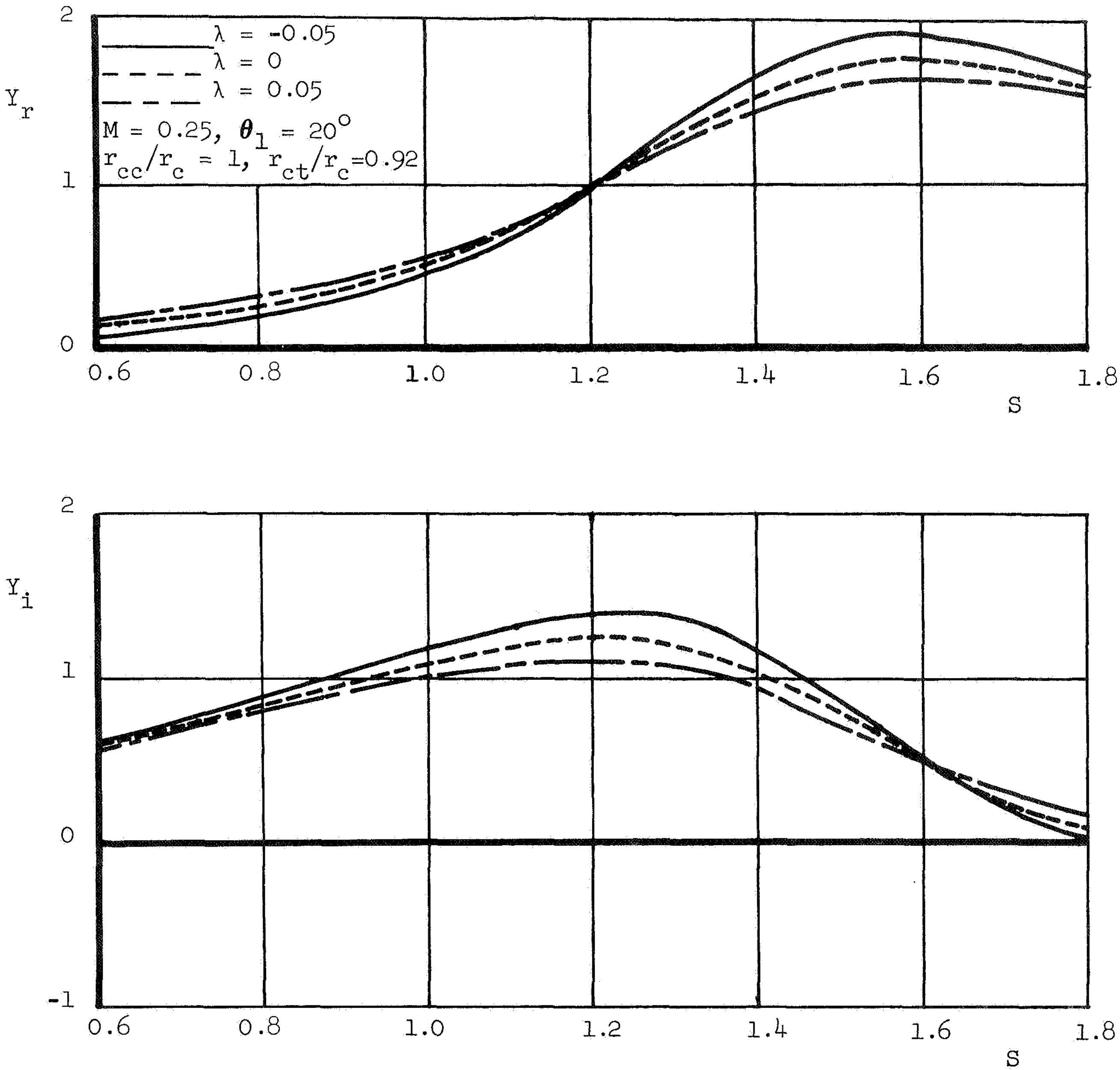

Figure 9. Effect of the Temporal Decay Coefficient on the Theoretical Nozzle Admittance Values for Longitudinal Modes

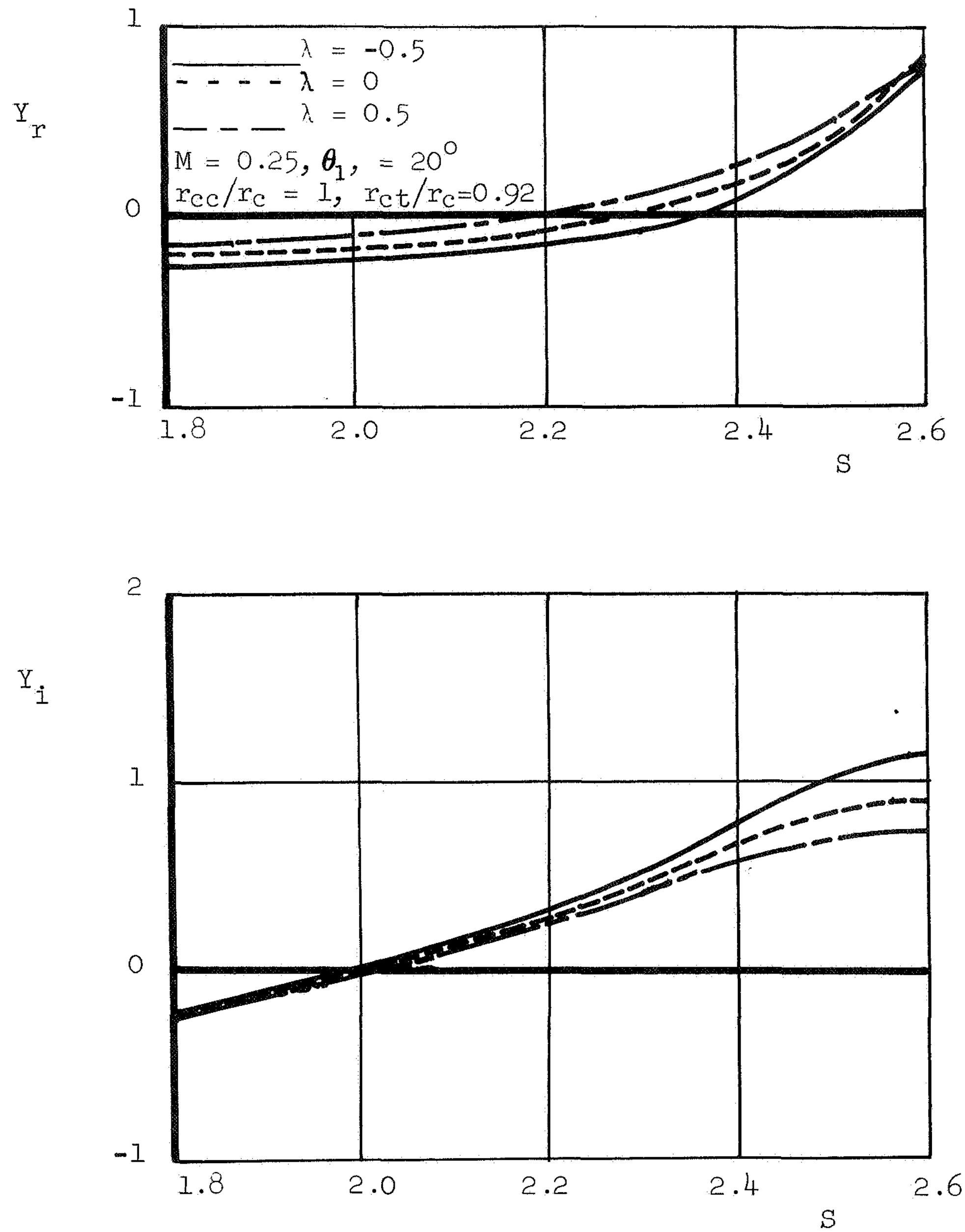

Figure 10. Effect of the Temporal Decay Coefficient on the Theoretical Nozzle Admittance Values for Mixed First Tangential-Longitudinal Modes

APPENDIX

COMPUTER PROGRAM USED TO DETERMINE THE IRROTATIONAL NOZZLE ADMITTANCE

The computer program for calculating the irrotational nozzle admittance from Crocco's theory[2] which is extended to account for temporal damping is written in FORTRAN V interpretive language compatible with the UNIVAC 1108 machine language compiler. This program consists of seven routines - the main or control program and six subroutines. The names of the routines are listed in Table A-1 in sequential order. The FORTRAN symbols used in these routines and their definitions are presented in Table A-2 in alphabetical order. The input parameters necessary for the admittance computations must be specified in the main program and are listed in Table A-3. The output parameters and their definitions are listed in Table A-4. A detailed flow chart of the computer program is shown in Fig. A-1, and the program listing and sample output are presented in Tables A-5 and A-6, respectively.

This computer program has been written to predict nozzle admittances for nozzle contours shown in Fig. 2. The run time required depends upon the number of admittance values desired and the nozzle length. To obtain 40 admittance values at different frequencies for the nozzles investigated in this study, one to two minutes of run time on the UNIVAC 1108 computer are required.

Table A-1. List of Subroutines in the Computer Program Used to Determine the Irrotational Nozzle Admittance

Subroutine	Description
MAIN	Specifies the nozzle geometry and operating conditions in the converging section of the nozzle
NOZADM	Specifies initial conditions at the throat, computes the final nozzle admittance values, and contains all output formats
RKTZ	Uses the Runge-Kutta of order four to obtain initial values for the modified Adams integration routine
RKZDIF	Computes the differential element in the converging section of the nozzle used to solve Eq. (14)
RKTDIF	Computes the differential element in the converging section of the nozzle used to solve Eq. (15)
ZADAMS	Numerically integrates Eq. (14) using the modified Adams numerical integration scheme
TADAMS	Numerically integrates Eq. (15) using the modified Adams numerical integration scheme

Table A-2. Definition of FORTRAN Variables
(Page 1 of 4)

Variable	Definition
A	Real coefficient A of Eqs. (14) and (15)
A(5)	Coefficients of the Runge-Kutta formulas of order four
AF	Nondimensional temporal damping coefficient λ
ANGLE	Nozzle half-angle, degrees
A1R	Derivative of the coefficient A evaluated at the throat
BI	Imaginary part of the coefficient B in Eqs. (14) and (15)
BR	Real part of the coefficient B in Eqs. (14) and (15)
BOI	Value of BI at the throat
BOR	Value of BR at the throat
B1I	Derivative of BI evaluated at the throat
B1R	Derivative of BR evaluated at the throat
C	Nondimensional speed of sound squared, c^2
CI	Imaginary part of the coefficient C in Eqs. (14) and (15)
CM	Mach number at the nozzle entrance
COR(5)	Formula for the corrector in the modified Adams integration routine
CR	Real part of the coefficient C in Eqs. (14) and (15)
COI	Value of CI at the throat
COR	Value of CR at the throat
C1I	Derivative of CI evaluated at the throat
C1R	Derivative of CR evaluated at the throat
DP	Integration stepsize
DP(5)	Derivative used in the corrector formula in the modified Adams integration routine
DR	Derivative of the local wall radius with respect to axial distance
DU	Derivative of the nondimensional velocity $\bar{q}^2$ with respect to the wall radius r
DWC	Increment of the nondimensional frequency ω

Table A-2. Definition of FORTRAN Variables
(Page 2 of 4)

Variable	Definition
DY(5,4)	Derivative used in the modified Adams integration scheme
F	Constant given as $\bar{q}/\gamma\bar{p}$ evaluated at the nozzle entrance
FZ(4,5)	Derivative used in the Runge-Kutta method
F1	Lumped parameter determined by the conditions at the throat
F2	Lumped parameter determined by the conditions at the throat
GAM	Ratio of specific heats γ
G(5)	Dependent variable in the Runge-Kutta integration routine
H	Integration stepsize
I	Integer counter
IP	Integer constant. If IP = 0 the nozzle admittance is output. If IP $\neq$ 0 the amplitude and phase of the pressure oscillation are output along the length of the nozzle
IQ	If IQ = 2, the integration of Eq. (15) for τ is complete
IQZ	= 1: Eq. (15) for τ is integrated = 2: Eq. (14) for ζ is integrated
J	Integer variable
JOPT	= 1: Eq. (15) for τ is integrated = 2: Eq. (14) for ζ is integrated
K	Integer variable
N	Integer variable
NU	Number of differential equations to be solved by the Runge-Kutta or the modified Adams integration routine
NWC	Number of frequency points
P	Value of the steady state velocity potential
PARG	Phase of the pressure oscillation in the nozzle
PHII	Imaginary part of Φ
PHIR	Real part of Φ

Table A-2. Definition of FORTRAN Variables
(Page 3 of 4)

Variable	Definition
PI	Imaginary part of the pressure oscillation
PMAG	Magnitude of the pressure oscillation
PR	Real part of the pressure oscillation
PRED(5)	Predictor formula for the modified Adams integration routine
Q	Constant given as $(r_{th}/4)\left(\frac{2}{\gamma + 1}\right)^{\frac{\gamma + 1}{4(\gamma - 1)}}$
QBAR	Nondimensional steady state velocity $\bar{q}$
R	Local wall radius r
RCC	Ratio of the radius of curvature at the nozzle entrance to the radius at the nozzle entrance
RCT	Ratio of the radius of curvature at the throat to the radius at the nozzle entrance
RHO	Nondimensional, steady-state density $\bar{\rho}$
RT	Nondimensional throat radius
R1	Nondimensional radius at the entrance to Section 2 of the converging portion of the nozzle
R2	Nondimensional radius at the entrance to Section 3 of the converging portion of the nozzle
SRTR	Constant give as $\sqrt{r_{th} r_{cc}}/r_c$
SVN	S_{mn}
SVNR	$S_{mn} r_c / r_{th}$
SYI	Imaginary part of the specific admittance y
SYR	Real part of the specific admittance y
T	Nozzle half-angle, in radians
TDN	Inverse of the square of the magnitude of ζ
TI	Imaginary part of τ
TMAG	Magnitude of τ
TPI	Derivative of TI with respect to φ

Table A-2. Definition of FORTRAN Variables
(Page 4 of 4)

Variable	Definition
TPR	Derivative of TR with respect to φ
TR	Real part of τ
TZ	Value of φ at the nth integration point
T2	Square of the magnitude of τ
U	Steady state velocity squared, $\bar{q}^2$
UZ	Dependent variable in the Runge-Kutta integration scheme
W	Nondimensional frequency S
WC	Nondimensional frequency ω
X	Value of φ at the nth integration point
Y(5)	Dependent variable used in the modified Adams integration scheme
YI	Imaginary part of the irrotational nozzle admittance defined by Crocco in Ref. 2
YR	Real part of the nozzle admittance defined by Crocco in Ref. 2
ZDN	Inverse of the square of the magnitude of ζ
ZI	Imaginary part of ζ
ZMAG	Magnitude of ζ
ZPI	Derivative of ZI with respect to φ
ZPR	Derivative of ZR with respect to φ
ZR	Real part of ζ
ZOI	Value of ZI at the throat
ZOR	Value of ZR at the throat
Z1I	Value of ZPI at the throat
Z1R	Value of ZPR at the throat
Z2	Square of the magnitude of ζ

Table A-3. Input Parameters

Variable	Definition
GAM	Ratio of specific heats, γ
CM	Mach number at the nozzle entrance
SVN	Nth root of the equation $\frac{dJ_V(x)}{dx} = 0$. Corresponds to S_{mn}. Values of S_{mn} are given in Table 1 for various acoustic modes
WC	Initial value of ω
DWC	Increment of frequency
NWC	Number of frequency points desired
ANGLE	Nozzle half-angle, degrees
RCT	Radius of curvature at the throat nondimensionalized with respect to the chamber radius
RCC	Radius of curvature at the nozzle entrance nondimensionalized with respect to the chamber radius
IP	$= 0$: nozzle admittances are printed $\neq 0$: pressure magnitude and phase are printed at each point along the nozzle
AF	Temporal damping coefficient λ

Table A-4. Output Parameters

Variable	Definition
WC	Nondimensional frequency, ω
YR	Real part of the admittance as defined by Crocco in Ref. 2
YI	Imaginary part of the admittance as defined by Crocco in Ref. 2
W	Nondimensional frequency
SYR	Real part of the specific admittance y
SYI	Imaginary part of the specific admittance y

Table A-5. Listing of the Computer Program Used to Determine the Irrotational Nozzle Admittance (Page 1 of 10)

```
          COMMON/X1/GAM, SVN, ANGLE, RCT, RCC /X2/T,RT, Q, R1, R2, IP, WC,AF
          COMMON/X3/Z1R, Z1I
          COMMON/X4/ CM
          GAM = 1.233
          AF = 0
          IP=0
          RCC = 1
          RCT = 5.457*2/11.82
          NWC = 40
          DWC = 0.05
          ANGLE = 20
          CM = .25
          DO 100 I = 1,2
          IF(I.EQ.2) GO TO 5
          SVN = 0
          NWC = 27
          GO TO 20
        5 SVN = 1.84129
          NWC = 20
       20 CONTINUE
          DO 200 J = 1,3
          AF = 0.05*(J-2)
          IF (I .EQ.2) GO TO 25
          WC = 0.55
          GO TO 30
       25 WC = 1.55
       30 CONTINUE
          IF(IP .EQ. 0) GO TO 10
          WRITE(6, 1000) CM, SVN, GAM, ANGLE, RCT, RCC
       10 CALL NOZADM(CM,     NWC, DWC).
      200 CONTINUE
      100 CONTINUE
     1000 FORMAT(46X, 28HPRESSURE MAGNITUDE AND PHASE, //, 38X,
        1        14HMACH NUMBER = , F3.2, 7H SVN = , F6.4, 9H GAMMA = , F3.1
        2        , /, 22X, 15HNOZZLE ANGLE = , F4.1, 21H RADII OF CURVATURE:
        3        , 9HTHROAT = , F6.4, 12H ENTRANCE = , F6.4, //, 46X,
        4        2H X, 7X, 4HPMAG, 10X, 4HPARG, /)
          STOP
          END
```

```
      SUBROUTINE NOZADM(CM,      NWC, DWC)
      DIMENSION DY(5,4), G(5), GP(5), Y(5)
      COMMON/X1/GAM,SVN,ANGLE,RCT,RCC/X2/T,RT,Q,R1,R2,IP,WC, AF
      COMMON/X3/Z1R,Z1I
      DP = -0.001
       T = 3.1415927 * ANGLE / 180
      WRITE(6,1000) CM, SVN, GAM, AF, ANGLE, RCT, RCC
      DO 10 N = 1, NWC
20          WC = WC + DWC
25          RT =(CM**0.5)*((1+ (GAM-1)*CM*CM/2)**((-GAM-1)/(4*(GAM-1)))
     1              )*((2/(GAM+1))**((-GAM-1)/(4*(GAM-1))))
             Q = (0.25*RT)*((2/(GAM+1))**((GAM+1)/(4*(GAM-1))))
          PHIR = 1
          PHII = 0
            R1 = RT + RCT*(1 - COS(T))
            R2 = 1   - RCC*(1 - COS(T))
             R = RT
             P = 0
             U = 2 / (GAM+1)
          SRTR = (RT * RCT)**0.5
           A1R = -4 /((GAM+1)*SRTR)
           BOR = -A1R +4*AF/(GAM+1)
           BOI = 4 * WC /(GAM+1)
          SVNR = SVN/RT
           COR = WC * WC -((SVNR*SVNR) * 2 / (GAM+1))
     1           - AF*AF - 2*AF*(GAM-1)/((GAM+1)*SRTR)
           COI = -2 * WC * (GAM-1) / ((GAM+1)*SRTR) - 2*AF*WC
           B1R = (24 + 4*GAM)/(3*RCT*RT*(GAM+1)) - 8*AF/(SRTR*(GAM+1))
           B1I = 8 * WC / (SRTR*(GAM+1))
           C1R = 2 * (GAM - 1) * SVNR * SVNR /(SRTR * (GAM+1))
     1           - AF* (B1R+8*AF/(SRTR*(GAM+1)))*(GAM-1)*0.5
           C1I = -B1R * WC * (GAM - 1) * 0.5
           ZOR = (BOR*COR + BOI*COI) / (BOR*BOR + BOI*BOI)
           ZOI = (BOR*COI - BOI*COR) / (BOR*BOR + BOI*BOI)
            F1 = B1R*ZOR - B1I*ZOI - ZOR*ZOR*A1R + A1R*ZOI*ZOI - C1R
            F2 = B1I*ZOR + B1R*ZOI - 2*A1R*ZOI*ZOR - C1I
           Z1R = (F1*(A1R - BOR) - F2*BOI) / ((A1R-BOR)*(A1R-BOR) +
     1             BOI*BOI)
           Z1I = (F2*(A1R - BOR) + F1*BOI) / ((A1R-BOR)*(A1R-BOR) +
     1             BOI*BOI)
             C = U
          G(1) = U
          G(2) = ZOR
          G(3) = ZOI
          G(4) = PHIR * ZOR - PHII * ZOI
          G(5) = PHII * ZOR + ZOI * PHIR
        DY(1,1) = -A1R
        DY(2,1) = Z1R
        DY(3,1) = Z1I
        DY(4,1) = PHIR
        DY(5,1) = PHII
           IQZ = 2
          DO 30 I = 2,4
               CALL RKTZ(5,DP,P,G,GP,IQZ)
                  P = P + DP
                  U = G(1)
                 ZR = G(2)
                 ZI = G(3)
               PHIR = G(4)
               PHII = G(5)
```

Table A-5. Continued (Page 3 of 10)

```
                    DY(1,I) = GP(1)
                    DY(2,I) = GP(2)
                    DY(3,I) = GP(3)
                    DY(4,I) = GP(4)
   30               DY(5,I) = GP(5)
                 Y(1) = U
                 Y(2) = ZR
                 Y(3) = ZI
                 Y(4) = PHIR
                 Y(5) = PHII
                 CALL ZADAMS(5,DP,P,Y,DY,IQZ)
                 IF(IP .EQ. 1) GO TO 10
                    U = Y(1)
                   ZR = Y(2)
                   ZI = Y(3)
         PHIR = Y(4)
         PHII = Y(5)
                 QBAR = U**0.5
                    C = 1 - U*0.5*(GAM-1)
                  RHO = C**(1/(GAM-1))
                    F = QBAR / (GAM*RHO)
                 IF(IQZ .EQ. 1) GO TO 35
                  ZDN = (U*ZR+AF)*(U*ZR+AF) + (WC+U*ZI)*(WC+U*ZI)
                   YR = -(ZR*(U*ZR+AF) + ZI*(WC+U*ZI))*F/ZDN
                   YI = F*(WC*ZR - AF*ZI)/ZDN
                 GO TO 40
   35              TR = Y(2)
                   TI = Y(3)
                  TDN = (U+AF*TR-WC*TI)*(U+AF*TR-WC*TI)+(WC*TR)*(WC*TR)
                   YR = -F*(U-WC*TI+AF*TR)/TDN
                   YI = F*(WC*TR+AF*TI)/TDN
                   YI = F * WC * TR / TDN
   40             SYR = GAM*(C**((GAM+1)/(2*(GAM-1))))*YR
                  SYI = GAM*(C**((GAM+1)/(2*(GAM-1))))*YI
                    W = WC *(C**-.5)
   50            WRITE(6,1005) WC, YR, YI, W, SYR, SYI
   10 CONTINUE
 1000 FORMAT(1H1, 45X, 30HTHEORETICAL NOZZLE ADMITTANCES, //, 25X,
     1          14HMACH NUMBER = , F3.2, 7H SVN = , F6.4, 9H GAMMA = , F3.1
     1         ,21H DECAY COEFFICIENT = , F6.4, //,
     2          22X, 15HNOZZLE ANGLE = , F4.1, 2X, 21HRADII OF CURVATURE:
     3         ,    9HTHROAT = , F6.4, 12H ENTRANCE = , F6.4, //, 34X, 2HWC,
     4          7X, 2HYR, 8X, 2HYI, 8X, 1HW, 8X, 3HSYR, 8X, 3HSYI, /)
 1005 FORMAT(31X, F6.4, 5F10.5)
      RETURN
      END
```

```
      SUBROUTINE RKTZ(NU, H, T1, U, DUM, JOPT)
      COMMON/X2/T,RT,Q,R1,R2,IP,WC,AF
      DIMENSION U(5), A(5), UZ(5), FZ(4,5),DUM(5)
      A(1) = 0
      A(2) = 0
      A(3) = 0.5
      A(4) = 0.5
      A(5) = 1.0
        TZ = T1
      DO 10 J = 1, NU
          UZ(J) = U(J)
   10    DUM(J) = FZ(1,J)
      IF(JOPT .EQ. 2) GO TO 15
      CALL RKTDIF(TZ,UZ,DUM)
      GO TO 20
   15 CALL RKZDIF(TZ,UZ,DUM)
   20 DO 25 J = 1, NU
   25   FZ(1,J) = DUM(J)
      DO 30 I = 2,4
             TZ = T1 + A(I+1)*H
           DO 35 J = 1, NU
                UZ(J) = U(J) + A(I+1)*H*FZ(I-1,J)
   35          DUM(J) = FZ(I,J)
           IF(JOPT .EQ. 2) GO TO 40
           CALL RKTDIF(TZ,UZ,DUM)
           GO TO 45
   40      CALL RKZDIF(TZ,UZ,DUM)
   45      DO 50 J = 1, NU
   50         FZ(I,J) = DUM(J)
   30 CONTINUE
      DO 55 J = 1, NU
   55      U(J) = U(J) + H*(FZ(1,J)+2*(FZ(2,J)+FZ(3,J))+FZ(4,J)) / 6.0
      GO TO (60,65),JOPT
   60 CALL RKTDIF(TZ,U ,DUM)
      GO TO 70
   65 CALL RKZDIF(TZ,U ,DUM)
   70 IF(IP.EQ.0) GO TO 75
        PR = WC*U(5)- U(1)*DUM(4) - AF*U(4)
        PI = -WC*U(4) - U(1)*DUM(5) - AF*U(5)
      PMAG = SQRT(PR*PR + PI*PI)
      PARG = ATAN(PI/PR)
      WRITE(6,1000) TZ, PMAG, PARG
 1000 FORMAT(46X, F6.4, 1X, F10.5, 3X, F10.5)
   75 RETURN
      END
```

```
      SUBROUTINE RKZDIF(P,G,GP)
      COMMON/X1/GAM,SVN,ANGLE,RCT,RCC/X2/T,RT,Q,R1,R2,IP,WC,AF
      COMMON/X3/Z1R,Z1I
      DIMENSION G(5), GP(5)
         U = G(1)
        ZR = G(2)
        ZI = G(3)
      PHIR = G(4)
      PHII = G(5)
      IF(P) 15, 10, 15
   10 GP(1) = 4/((GAM+1)*((RCT*RT)**0.5))
      GP(2) = Z1R
      GP(3) = Z1I
      GP(4) = Z1R
      GP(5) = Z1I
      GO TO 20
   15    C = 1 - (GAM - 1) * U * 0.5
         R = Q * ((C)**(-1/(2*(GAM-1)))) * (U**-0.25) *4.0
      IF(R-1) 22, 22, 50
   22 IF(R - R1) 25, 30, 30
   25    DR = -((2*RCT*(R-RT) - (R-RT)*(R-RT))**0.5)/(RT+RCT-R)
      GO TO 45
   30 IF(R-R2) 35, 40, 40
   35    DR = -TAN(T)
      GO TO 45
   40    DR = ((2*RCC*(1-R) - (R-1)*(R-1))**0.5)/(1-R-RCC)
   45    DU = -(U**0.75)*(C**((2*GAM-1)/(2*(GAM-1))))/(Q*(1-(GAM+1)*U*.5)
     1         )
      GP(1)= DU*DR
      GO TO 55
   50 GP(1) = 0
   55     A = U*(C-U)
         BR = U*GP(1)/C + 2*AF*U
         BI = 2*WC*U
         CR = WC*WC - SVN*SVN*C/(R*R) - AF*AF
     1          -(GAM-1)*AF*U*GP(1)*0.5*(1/C)
         CI = -(GAM-1)*WC*U*GP(1)*0.5*(1/C) - 2*AF*WC
      GP(2)= ((BR*ZR - BI*ZI - CR) / A) - ZR*ZR + ZI*ZI
      GP(3)= ((BI*ZR + BR*ZI - CI) / A) - 2*ZR*ZI
      GP(4)= ZR*PHIR - ZI*PHII
      GP(5)= ZR*PHII + ZI*PHIR
   20 RETURN
      END
```

```
      SUBROUTINE RKTDIF(P,G,GP)
      COMMON/X1/GAM,SVN,ANGLE,RCT,RCC/X2/T,RT,Q,R1,R2,IP,WC,AF
      DIMENSION G(5), GP(5)
         U = G(1)
        TR = G(2)
        TI = G(3)
      PHIR = G(4)
      PHII = G(5)
         C = 1 - (GAM-1)*U*0.5
         R = Q * ((C)**(-1/(2*(GAM-1)))) * (U**-0.25) *4.0
      IF(R-1) 22,22,50
   22 IF(R-R1) 25, 30, 30
   25   DR = -((2*RCT*(R-RT) - (R-RT)*(R-RT))**0.5)/(RT+RCT-R)
      GO TO 45
   30 IF(R-R2) 35,40,40
   35   DR = -TAN(T)
      GO TO 45
   40   DR = ((2*RCC*(1-R) - (R-1)*(R-1))**0.5)/(1-R-RCC)
   45   DU = -(U**0.75)*(C**((2*GAM-1)/(2*(GAM-1)))) / (Q*(1-(GAM+1)*U*
     1         0.5))
      GP(1)= DU*DR
      GO TO 55
   50 GP(1) = 0
   55    A = U*(C-U)
        BR = U*GP(1)/C + 2*AF*U
        BI = 2*WC*U
        CR = WC*WC - SVN*SVN*C/(R*R) - AF*AF
     1       -(GAM-1)*AF*U*GP(1)*0.5*(1/C)
        CI = -(GAM-1)*WC*U*GP(1)*0.5*(1/C) - 2*AF*WC
      GP(2)= 1 - (BR*TR-BI*TI) - (CR*(TR*TR-TI*TI)-2*CI*TR*TI))/ A
      GP(3)= (-BR*TI - BI*TR + CI*(TR*TR-TI*TI) + 2*CR*TR*TI) /A
        T2 = TR*TR + TI*TI
      GP(4)= (TR*PHIR - TI*PHII)/T2
      GP(5)= (TR*PHII + TI*PHIR)/T2
      RETURN
      END
```

```
      SUBROUTINE ZADAMS(N,H,X,Y,DY,IQZ)
      COMMON/X1/GAM,SVN,ANGLE,RCT,RCC/X2/T,RT,Q,R1,R2,IP,WC,AF
      COMMON/X4/ CM
      DIMENSION COR(5), DP(5), DY(5,4), PRED(5), Y(5), Q(5), GP(5)
   10 CONTINUE
      DO 15 I = 1,N
        PRED(I) = Y(I)+H*(55.*DY(I,4)-59.*DY(I,3)+37.*DY(I,2)-9.*DY(I,1)
     1                    )/24.0
   15 CONTINUE
         X = X+H
         U = PRED(1)
        ZR = PRED(2)
        ZI = PRED(3)
      PHIR = PRED(4)
      PHII = PRED(5)
         C = 1 - (GAM-1)*U*0.5
         R = Q * ((C)**(-1/(2*(GAM-1)))) * (U**-0.25) *4.0
      IF(R-1) 17,17,100
   17 IF(R-R1) 20, 25, 25
   20   DR = -((2*RCT*(R-RT)-(R-RT)*(R-RT))**0.5) / (RT+RCT-R)
      GO TO 40
   25 IF(R-R2) 30, 35, 35
   30   DR = -TAN(T)
      GO TO 40
   35   DR = ((2*RCC*(1-R) - (1-R)*(1-R))**0.5) / (1-R-RCC)
   40   DU = -(U**0.75)*(C**((2*GAM-1)/(2*(GAM-1))))/(Q*(1-(GAM+1)*U*0.5
     1           ))
      DP(1)= DR*DU
         A = U*(C-U)
        BR = U*DP(1)/C+ 2*AF*U
        BI = 2*WC*U
        CR = WC*WC - (SVN*SVN*C)/(R*R) - AF*AF
     1         -(GAM-1)*AF*U*DP(1)*0.5/C
        CI = -(GAM-1)*WC*U*DP(1)*0.5/C - 2*AF*WC
      DP(2)= ((BR*ZR - BI*ZI - CR)/A) - ZR*ZR + ZI*ZI
      DP(3)= ((BI*ZR + BR*ZI - CI)/A) - 2*ZR*ZI
      DP(4)= ZR*PHIR - ZI*PHII
      DP(5)= ZR*PHII + ZI*PHIR
      DO 45 I = 1,N
         COR(I) = Y(I)+H*(DY(I,2)-5.*DY(I,3)+19.*DY(I,4)+9.*DP(I))/24.0
   45      Y(I) = (251.*COR(I) + 19.*PRED(I)) / 270.
         U = Y(1)
        ZR = Y(2)
        ZI = Y(3)
      PHIR = Y(4)
      PHII = Y(5)
         C = 1 - (GAM-1)*U*0.5
   52 DO 55 I = 1,N
        DY(I,1) = DY(I,2)
        DY(I,2) = DY(I,3)
   55   DY(I,3) = DY(I,4)
      ZMAG = (ZR*ZR + ZI*ZI)**0.5
      IF(ZMAG - 10 ) 60, 90, 90
   60    R = Q * ((C)**(-1/(2*(GAM-1)))) * (U**-0.25) *4.0
      IF(R-1) 62, 62, 100
   62 IF(R-R1) 65,70,70
   65   DR = -((2*RCT*(R-RT) - (R-RT)*(R-RT))**0.5)/(RT+RCT-R)
      GO TO 85
   70 IF(R-R2) 75,80,80
   75   DR = -TAN(T)
      GO TO 85
```

```
80    DR = ((2*RCC*(1-R) - (1-R)*(1-R))**0.5)/(1-R-RCC)
85    DU = -(U**0.75)*(C**((2*GAM-1)/(2*(GAM-1))))/(Q*(1-(GAM+1)*U/2))
     DY(1,4)= DR*DU
        A = U*(C-U)
       BR = U*DY(1,4)/C + 2*AF*U
       BI = 2*WC*U
       CR = WC*WC - (SVN*SVN*C)/(R*R) - AF*AF
    1          -(GAM-1)*AF*U*DY(1,4)*0.5/C
       CI = -(GAM-1)*WC*U*DY(1,4)*0.5/C -2*AF*WC
     DY(2,4)= (BR*ZR - BI*ZI -CR)/A - ZR*ZR + ZI*ZI
     DY(3,4)= (BI*ZR + BR*ZI -CI)/A - 2*ZR*ZI
     DY(4,4)= ZR*PHIR - ZI*PHII
     DY(5,4)= ZR*PHII + ZI*PHIR
     IF(IP .EQ. 0) GO TO 87
       PR = WC*PHII - U*DY(4,4) - AF*PHIR
       PI = -WC*PHIR -U*DY(5,4)    - AF*PHII
     PMAG = (PR*PR + PI*PI)**.5
     PARG = ATAN(PI/PR)
     WRITE(6,1000) X, PMAG, PARG
87   GO TO 10
90    IQZ = 1
       Z2 = ZMAG*ZMAG
     Y(2) = ZR/Z2
     Y(3) = -ZI/Z2
      ZPR = DY(2,4)
      ZPI = DY(3,4)
     DY(2,4)= -(ZPR*(ZR*ZR - ZI*ZI) + 2*ZR*ZI*ZPI)/(Z2*Z2)
     DY(3,4)= (2*ZPR*ZR*ZI - ZPI*(ZR*ZR - ZI*ZI))/(Z2*Z2)
     G(1) = U
     G(2) = Y(2)
     G(3) = Y(3)
     G(4) = PHIR
     G(5) = PHII
     DY(1,1)= DY(1,4)
     DY(2,1)= DY(2,4)
     DY(3,1)= DY(3,4)
     DY(4,1)= PHIR*ZR - PHII*ZI
     DY(5,1)= PHII*ZR + PHIR*ZI
     DO 95 I = 2,4
          CALL RKTZ(5,H,X,G,GP,IQZ)
                X = X+H
                U = G(1)
               TR = G(2)
               TI = G(3)
             PHIR = G(4)
             PHII = G(5)
         DY(1,I) = GP(1)
         DY(2,I) = GP(2)
         DY(3,I) = GP(3)
         DY(4,I) = GP(4)
95       DY(5,I) = GP(5)
     Y(1) = U
     Y(2) = TR
     Y(3) = TI
     Y(4) = PHIR
     Y(5) = PHII
     CALL TADAMS(N,H,X,Y,DY,IQZ,IQ)
     GO TO (10, 100),IQ
1000 FORMAT(46X,F6.4,1X,F10.5,3X,F10.5)
100  RETURN
     END
```

```
      SUBROUTINE TADAMS(N,H,X,Y,DY,IQZ,IQ)
      COMMON/X1/GAM,SVN,ANGLE,RCT,RCC/X2/T,RT,Q,R1,R2,IP,WC,AF
      COMMON/X4/ CM
      DIMENSION COR(5), DP(5), DY(5,4), PRED(5), Y(5), G(5), GP(5)
   10 CONTINUE
      DO 15 I = 1,N
        PRED(I) = Y(I)+H*(55*DY(I,4)-59.*DY(I,3)+37.*DY(I,2)-9*DY(I,1))/
     1            24.0
   15 CONTINUE
          X = X+H
          U = PRED(1)
         TR = PRED(2)
         TI = PRED(3)
       PHIR = PRED(4)
       PHII = PRED(5)
          C = 1 - (GAM-1)*U*.5
          R = Q * ((C)**(-1/(2*(GAM-1)))) * (U**-0.25) *4.0
      IF(R-1) 17,17,100
   17 IF(R-R1) 20, 25, 25
   20   DR = -((2*RCT*(R-RT) - (R-RT)*(R-RT))**.5)/(RT+RCT-R)
      GO TO 40
   25 IF(R-R2) 30, 35, 35
   30   DR = -TAN(T)
      GO TO 40
   35   DR = ((2*RCC*(1-R) - (1-R)*(1-R))**.5)/(1-R-RCC)
   40   DU =-(U**.75)*(C**((2*GAM-1)/(2*(GAM-1))))/(Q*(1-(GAM+1)*U*.5))
      DP(1)= DR*DU
          A = U*(C-U)
         BR = U*DP(1)/C+ 2*AF*U
         BI = 2*WC*U
         CR = WC*WC - (SVN*SVN*C)/(R*R) - AF*AF
     1        -(GAM-1)*AF*U*DP(1)*0.5/C
         CI = -(GAM-1)*WC*U*DP(1)*0.5/C - 2*AF*WC
      DP(2)= 1 + (-BR*TR+BI*TI+CR*(TR*TR-TI*TI)-2*CI*TR*TI)/A
      DP(3)= (-BR*TI - BI*TR + CI*(TR*TR - TI*TI) + 2*CR*TR*TI)/A
         T2 = TR*TR + TI*TI
      DP(4)= (TR*PHIR - TI*PHII)/T2
      DP(5)= (TR*PHII + TI*PHIR)/T2
      DO 45 I = 1,N
          COR(I) = Y(I)+H*(DY(I,2)-5.*DY(I,3)+19.*DY(I,4)+9.*DP(I))/24.0
   45        Y(I) = (251.*COR(I) + 19.*PRED(I))/270.
          U = Y(1)
         TR = Y(2)
         TI = Y(3)
       PHIR = Y(4)
       PHII = Y(5)
          C = 1 - (GAM-1)*U*.5
   52 DO 55 I = 1,N
        DY(I,1) = DY(I,2)
        DY(I,2) = DY(I,3)
   55   DY(I,3) = DY(I,4)
         T2 = TR*TR + TI*TI
       TMAG = T2**.5
      IF(TMAG - 10 ) 60, 90, 90
   60     R = Q * ((C)**(-1/(2*(GAM-1)))) * (U**-0.25) *4.0
      IF(R-1) 62, 62, 100
   62 IF(R-R1) 65,70,70
   65   DR = -((2*RCT*(R-RT)-(R-RT)*(R-RT))**.5)/(RT+RCT-R)
      GO TO 85
   70 IF(R-R2) 75,80,80
   75   DR = -TAN(T)
      GO TO 85
```

```
 80   DR = ((2*R*C*(1-R) - (1-R)*(1-R))**.5)/(1-R-RCC)
 85   DU = -(U**.75)*(C**((2*GAM-1)/(2*(GAM-1))))/(Q*(1-(GAM+1)*U*.5)
      DY(1,4)= DR*DU
        A = U*(C-U)
        BR = U*DY(1,4)/C + 2*AF*U
        BI = 2*WC*U
        CR = WC*WC - (SVN*SVN*C)/(R*R) - AF*AF
     1          -(GAM-1)*AF*U*DY(1,4)*0.5/C
        CI = -(GAM-1)*WC*U*DY(1,4)*0.5/C -2*AF*WC
      DY(2,4)= 1 + (-BR*TR + BI*TI + CR*(TR*TR - TI*TI) - 2*CI*TR*TI)/A
      DY(3,4)= (-BR*TI - BI*TR + CI*(TR*TR - TI*TI) + 2*CR*TR*TI)/A
      DY(4,4)= (TR*PHIR - PHII*TI)/T2
      DY(5,4)= (TR*PHII + PHIR*TI)/T2
      IF(IP .EQ. 0) GO TO 87
        PR = WC*PHII - U*DY(4,4) - AF*PHIR
        PI = -WC*PHIR -U*DY(5,4)    - AF*PHII
      PMAG = (PR*PR + PI*PI)**.5
      PARG = ATAN(PI/PR)
      WRITE(6,1000) X, PMAG, PARG
 87   GO TO 10
 90    IQZ = 2
      Y(2) = TR/T2
      Y(3) = -TI/T2
       TPR = DY(2,4)
       TPI = DY(3,4)
      DY(2,4)= -(TPR*(TR*TR - TI*TI) + 2*TR*TI*TPI)/(T2*T2)
      DY(3,4)=(2*TPR*TR*TI-TPI*(TR*TR-TI*TI))/(T2*T2)
      G(1) = U
      G(2) = Y(2)
      G(3) = Y(3)
      G(4) = PHIR
      G(5) = PHII
      DY(1,1)= DY(1,4)
      DY(2,1)= DY(2,4)
      DY(3,1)= DY(3,4)
      DY(4,1)= (PHIR*TR - PHII*TI)/T2
      DY(5,1)= (PHII*TR - PHIR*TI)/T2
      DO 95 I = 2,4
            CALL RKTZ(5,H,X,G,GP,IQZ)
                X = X+H
                U = G(1)
               ZR = G(2)
               ZI = G(3)
             PHIR = G(4)
             PHII = G(5)
        DY(1,I) = GP(1)
        DY(2,I) = GP(2)
        DY(3,I) = GP(3)
        DY(4,I) = GP(4)
 95     DY(5,I) = GP(5)
      Y(1) = U
      Y(2) = ZR
      Y(3) = ZI
      Y(4) = PHIR
      Y(5) = PHII
       IQ  = 1
      GO TO 105
 100    IQ = 2
 1000 FORMAT(46X, F6.4, 1X, F10.5, 3X, F10.5)
 105  RETURN
      END
```

Table A-6. Sample Output

THEORETICAL NOZZLE ADMITTANCES

MACH NUMBER = .25 SVN = 1.8413 GAMMA = 1.2 DECAY COEFFICIENT = -.0500

NOZZLE ANGLE = 20.0 RADII OF CURVATURE: THROAT = .9234 ENTRANCE = 1.0000

WC	YR	YI	W	SYR	SYI
1.6000	-.28273	-.35883	1.60581	-.33670	-.42732
1.6500	-.27001	-.31495	1.65600	-.32154	-.37507
1.7000	-.25820	-.27057	1.70618	-.30749	-.32221
1.7500	-.24715	-.22543	1.75636	-.29433	-.26845
1.8000	-.23669	-.17922	1.80654	-.28186	-.21343
1.8500	-.22661	-.13161	1.85672	-.26986	-.15673
1.9000	-.21667	-.08219	1.90690	-.25803	-.09788
1.9500	-.20659	-.03048	1.95709	-.24603	-.03630
2.0000	-.19598	.02407	2.00727	-.23339	.02867
2.0500	-.18432	.08216	2.05745	-.21950	.09784
2.1000	-.17087	.14458	2.10763	-.20348	.17217
2.1500	-.15459	.21227	2.15781	-.18410	.25279
2.2000	-.13397	.28633	2.20799	-.15954	.34098
2.2500	-.10675	.36791	2.25818	-.12713	.43814
2.3000	-.06962	.45811	2.30836	-.08291	.54555
2.3500	-.01763	.55747	2.35854	-.02100	.66387
2.4000	.05634	.66508	2.40872	.06709	.79202
2.4500	.16198	.77657	2.45890	.19290	.92479
2.5000	.31059	.88072	2.50908	.36987	1.04883
2.5500	.49682	.94690	2.55927	.59165	1.12657

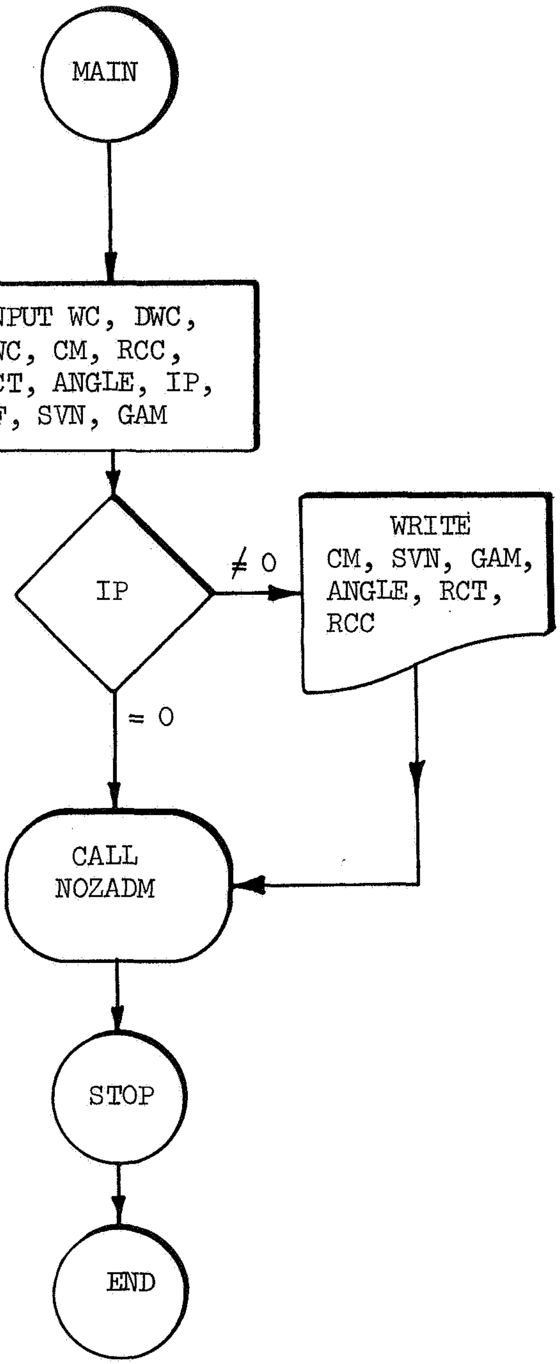

Figure A-1. Flow Chart for the Nozzle Admittance Computer Program (Page 1 of 10)

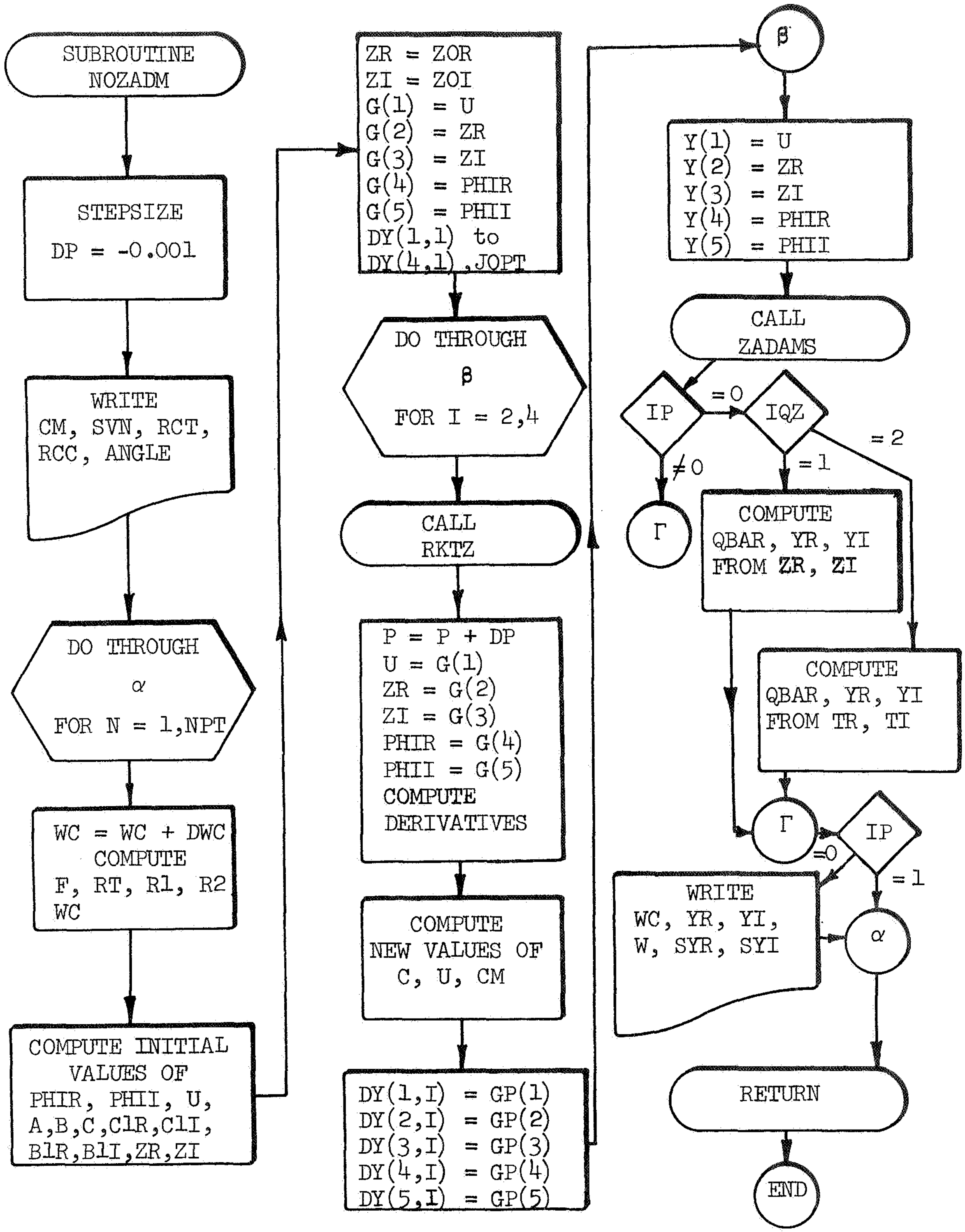

Figure A-1. Continued (Page 2 of 10)

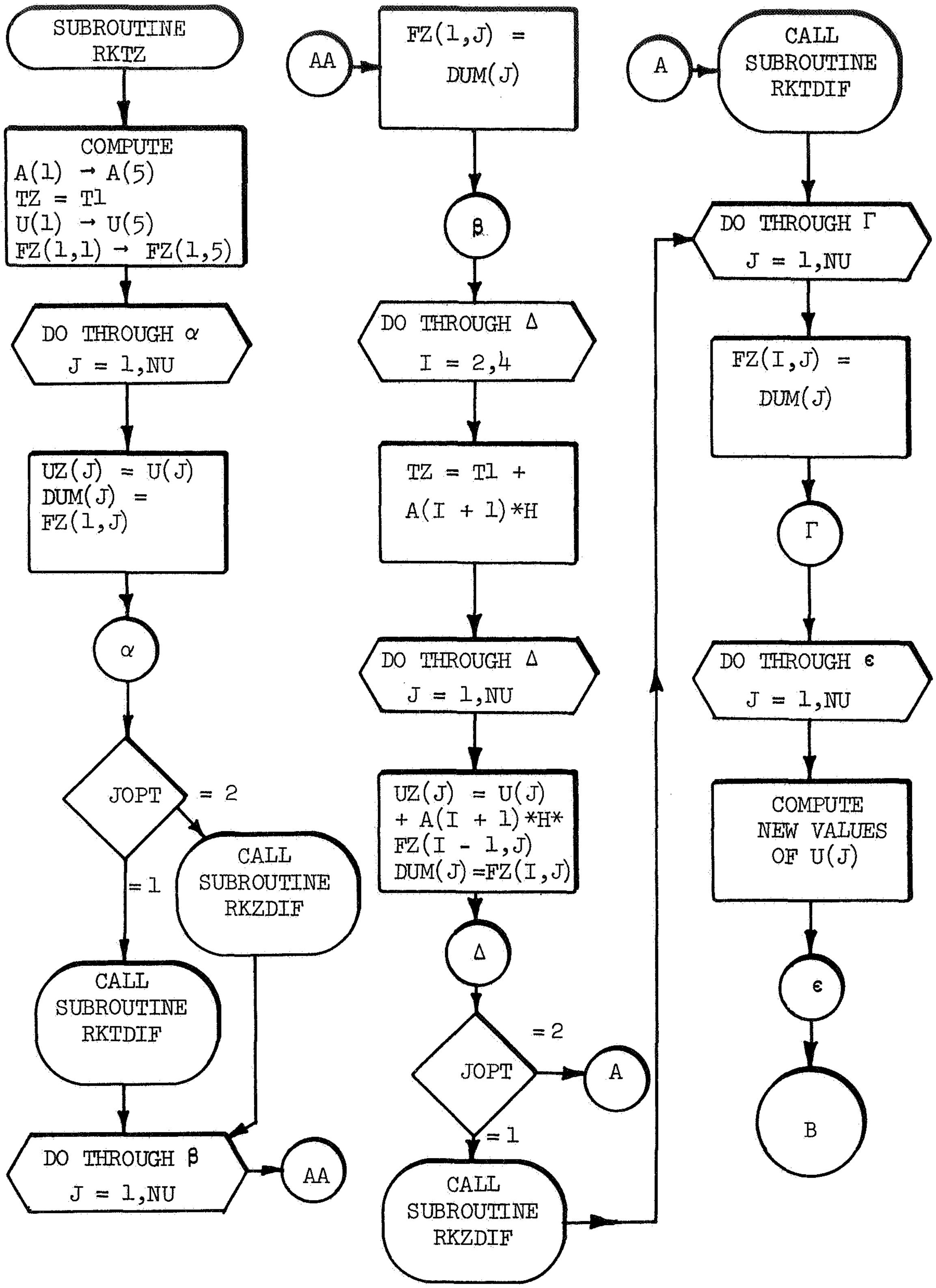

Figure A-1. Continued (Page 3 of 10)

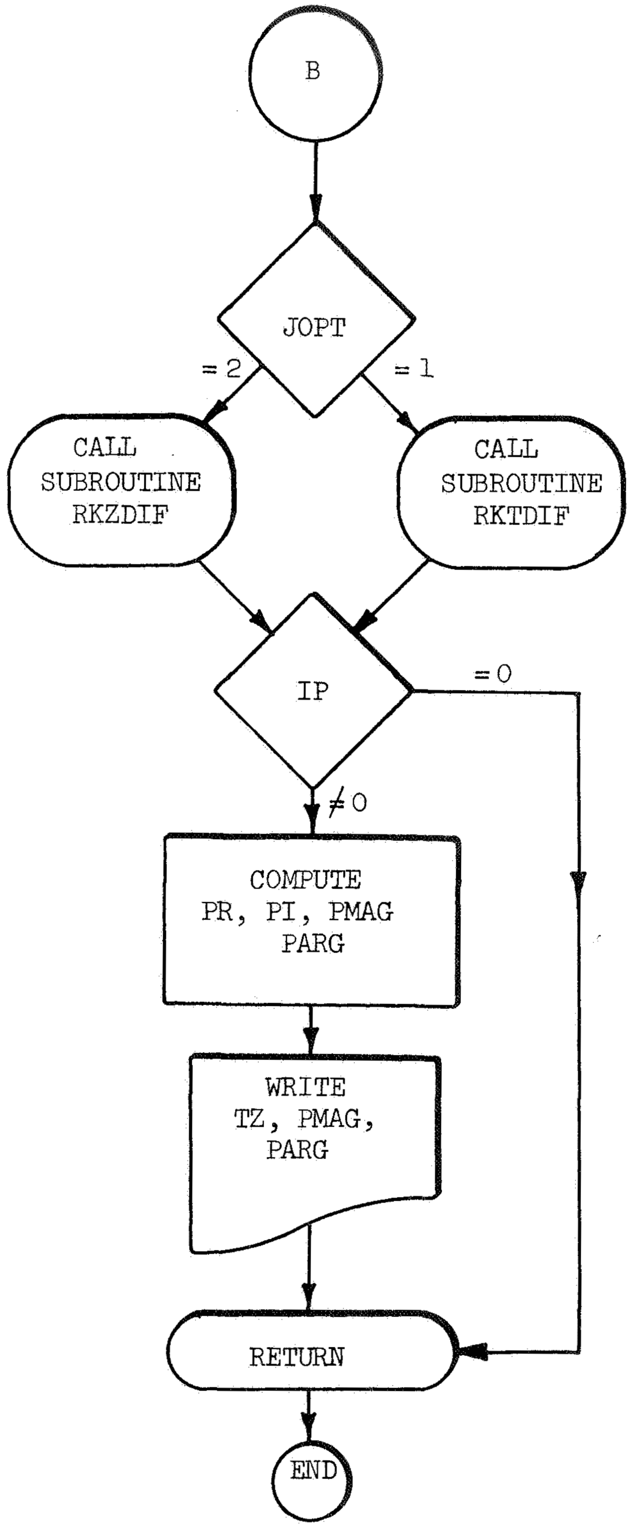

Figure A-1. Continued (Page 4 of 10)

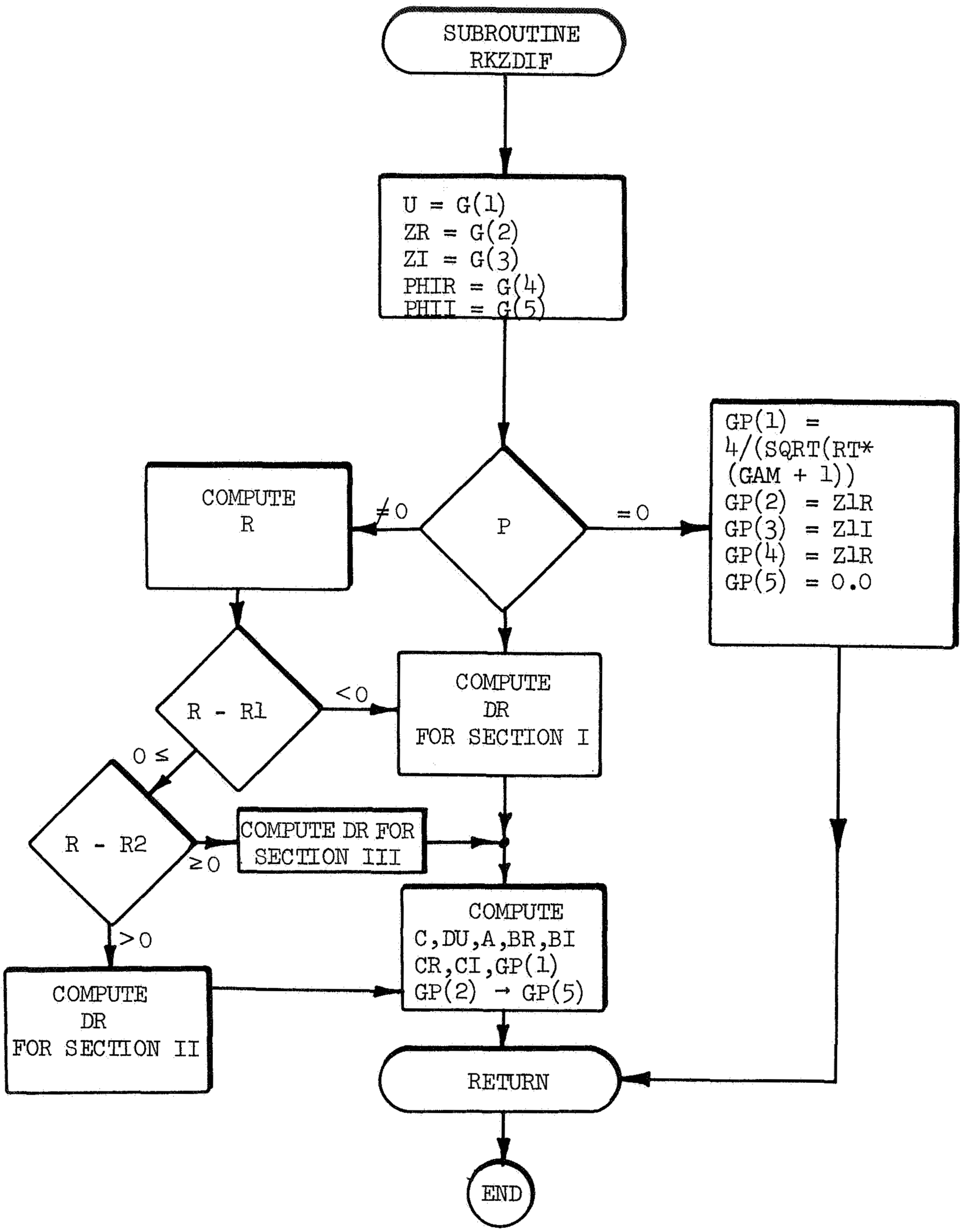

Figure A-1. Continued (Page 5 of 10)

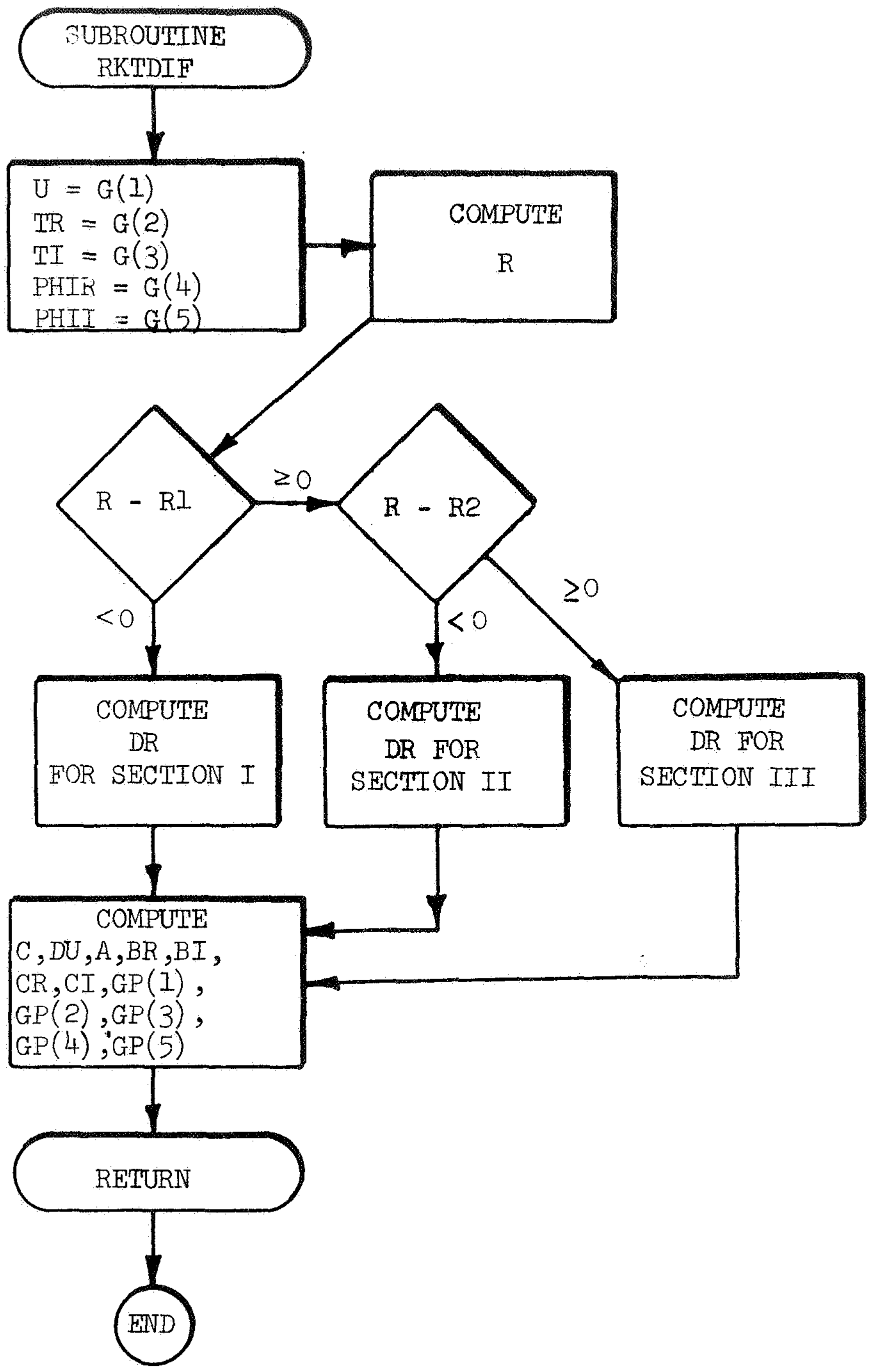

Figure A-1. Continued (Page 6 of 10)

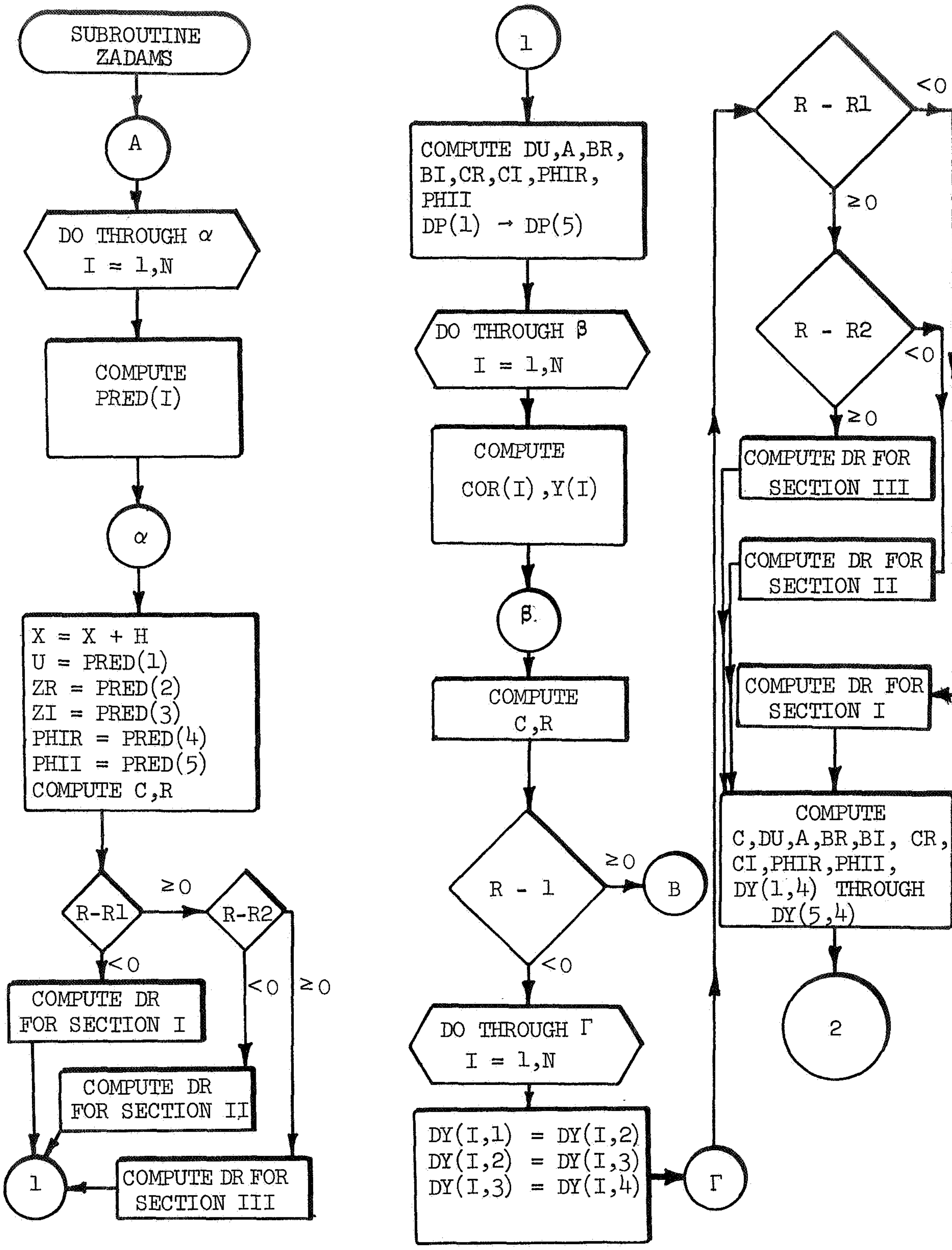

Figure A-1. Continued (Page 7 of 10)

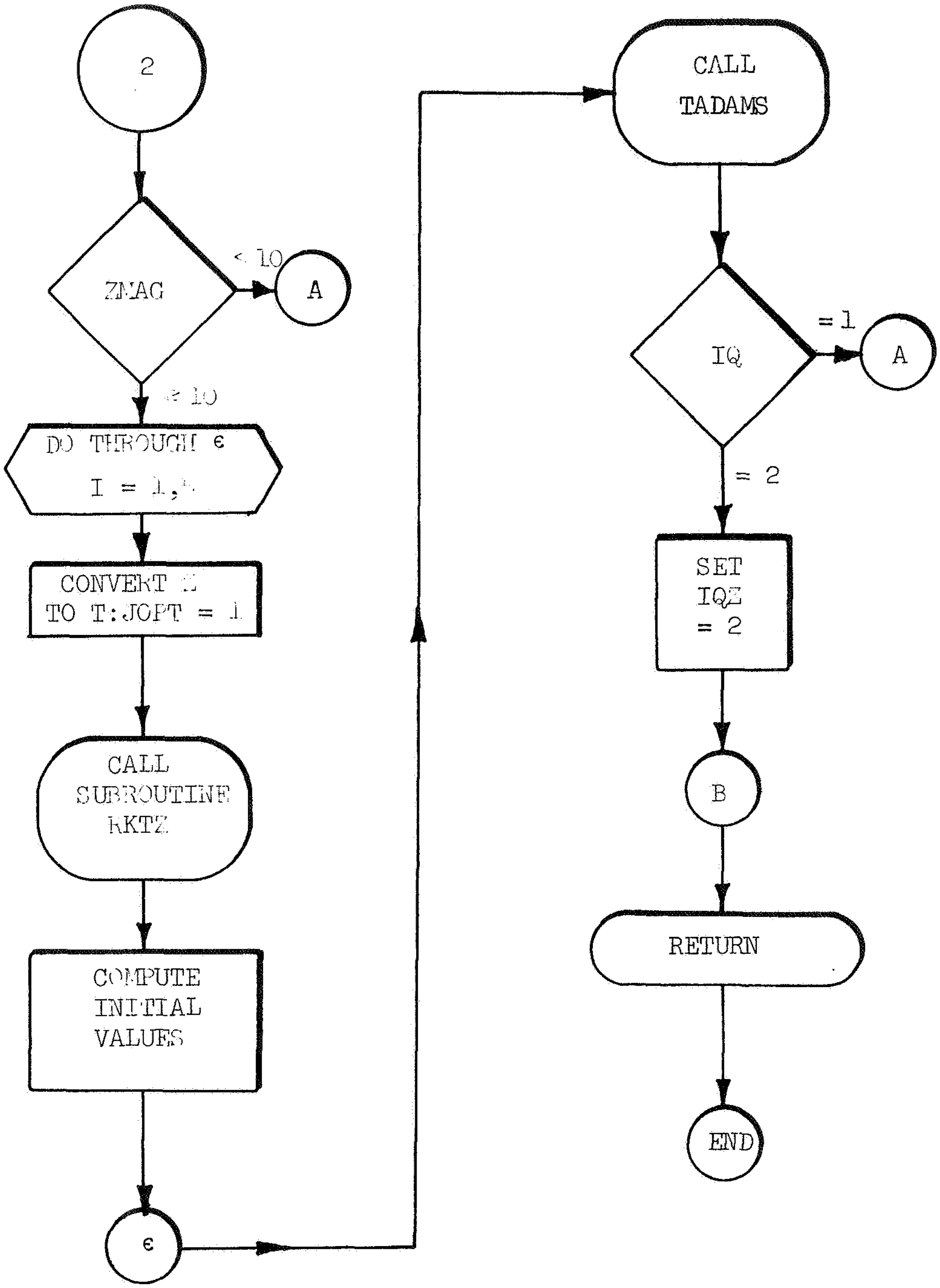

Figure A-1. Continued (Page 8 of 10)

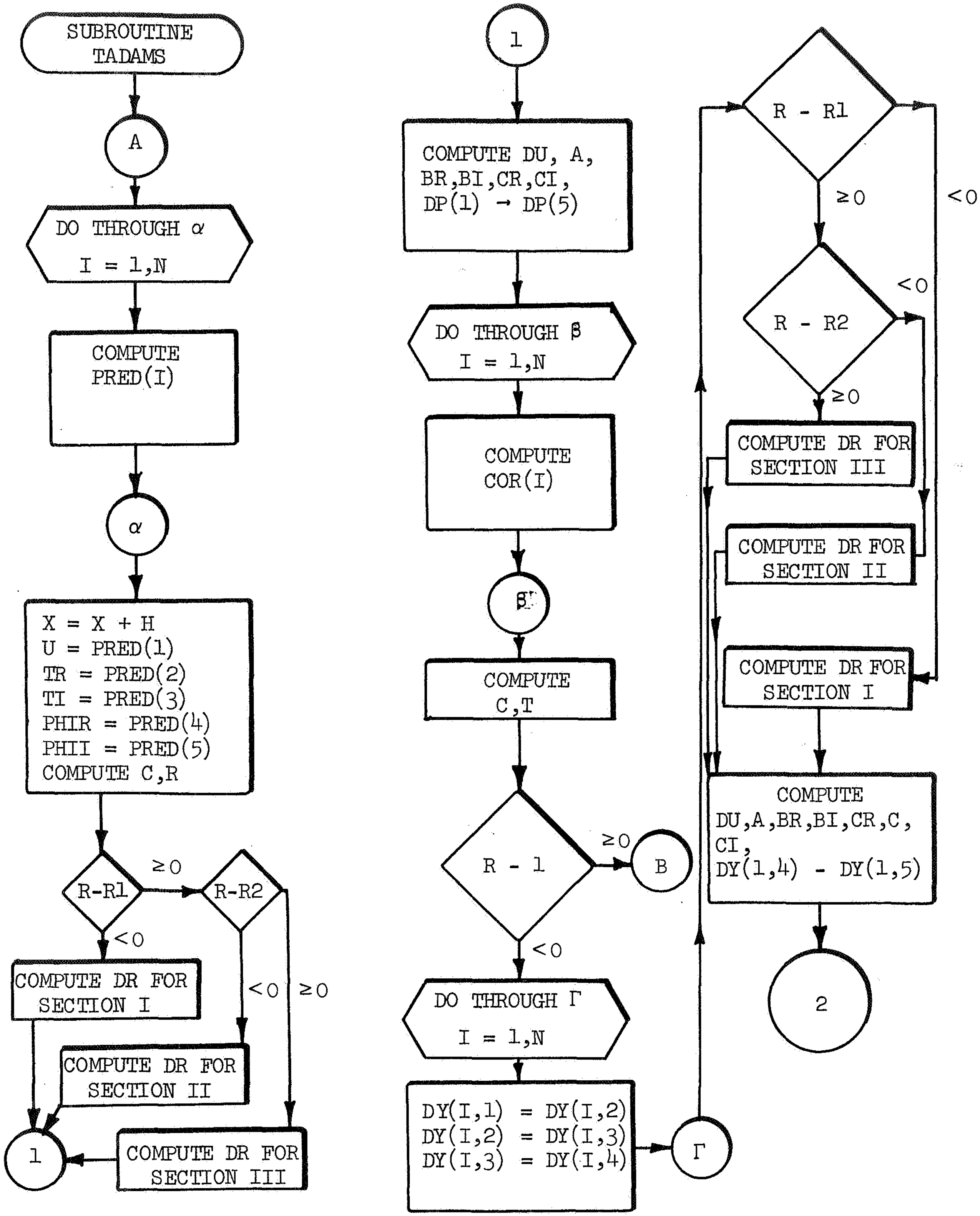
SUBROUTINE TADAMS
A
DO THROUGH α I = 1,N
COMPUTE PRED(I)
α
X = X + H
U = PRED(1)
TR = PRED(2)
TI = PRED(3)
PHIR = PRED(4)
PHII = PRED(5)
COMPUTE C,R
R-R1
≥0
<0
R-R2
<0
≥0
COMPUTE DR FOR SECTION I
COMPUTE DR FOR SECTION II
COMPUTE DR FOR SECTION III
1
1
COMPUTE DU, A, BR,BI,CR,CI, DP(1) → DP(5)
DO THROUGH β I = 1,N
COMPUTE COR(I)
β
COMPUTE C,T
R - 1
≥0
B
<0
DO THROUGH Γ I = 1,N
DY(I,1) = DY(I,2)
DY(I,2) = DY(I,3)
DY(I,3) = DY(I,4)
Γ
R - R1
≥0
<0
R - R2
<0
≥0
COMPUTE DR FOR SECTION III
COMPUTE DR FOR SECTION II
COMPUTE DR FOR SECTION I
COMPUTE DU,A,BR,BI,CR,C, CI, DY(1,4) - DY(1,5)
2

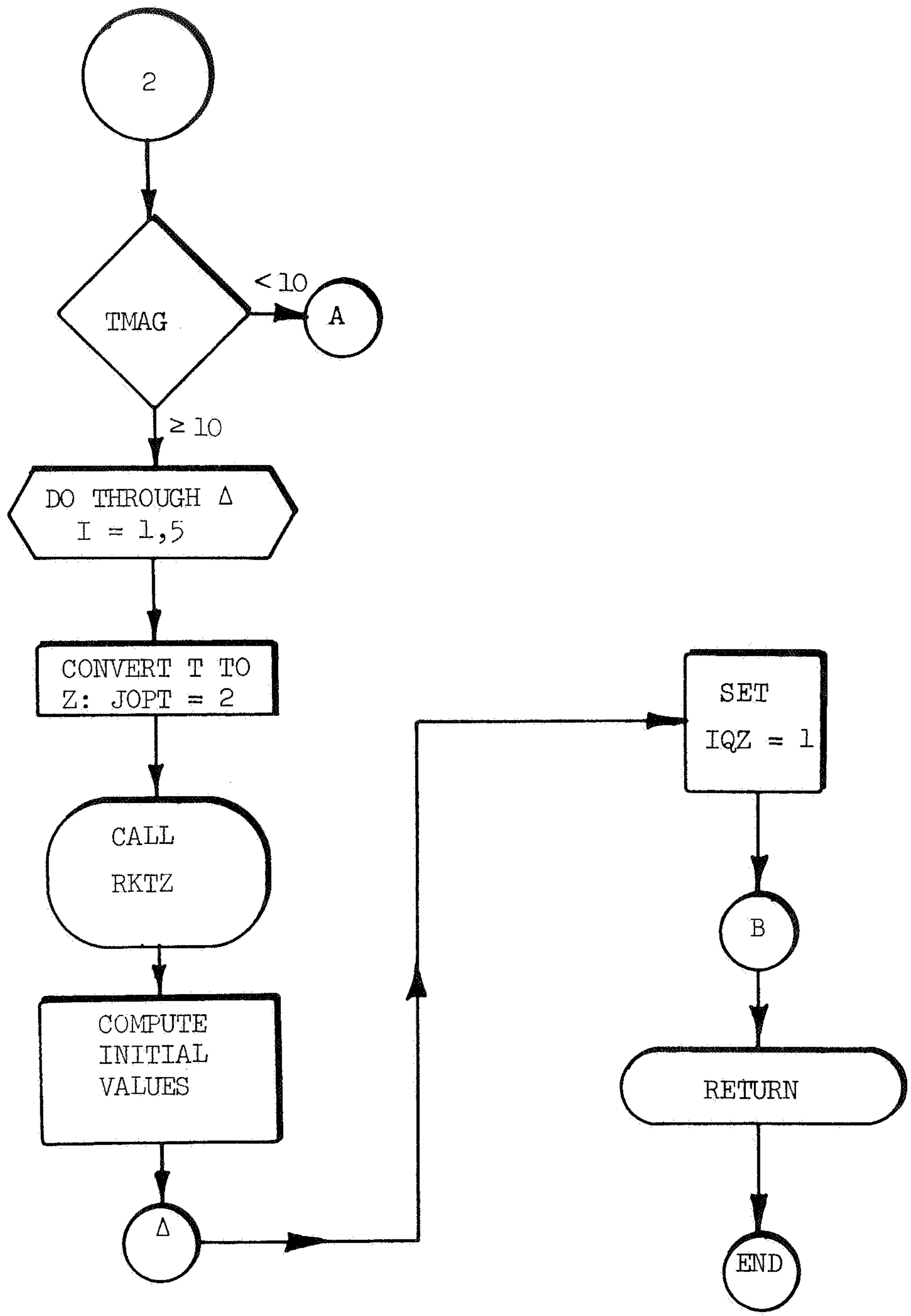

Figure A-1. Concluded (Page 10 of 10)

REFERENCES

1. Crocco, L., and Cheng, S. I., Theory of Combustion Instability in Liquid Propellant Rocket Motors , AGARDograph 8, Butterworth Publications Limited, London, 1956.
2. Crocco, L., and Sirignano, W. A., Behavior of Supercritical Nozzles under Three-Dimensional Oscillatory Conditions, AGARDograph 117, Butterworth Publications Limited, London, 1967.
3. Bell, W. A., "Experimental Determination of Three-Dimensional Liquid Rocket Nozzle Admittances," PH.D. Thesis, School of Aerospace Engineering, Georgia Institute of Technology, Atlanta, Georgia, July 1972.
4. Serra, R. A., "Determination of Internal Gas Flows by a Transient Numerical Technique," AIAA Journal, Vol. 10, May 1972, p. 603.
5. Zinn, B. T., "Longitudinal Mode Acoustic Losses in Short Nozzles," J. of Sound and Vibration, 22(1), pp. 93-105, 1972.

REPORT DISTRIBUTION LIST

Dr. R. J. Priem, MS 500-209
NASA Lewis Research Center
21000 Brookpark Road
Cleveland, Ohio 44135 (2)

Norman T. Musial
NASA Lewis Research Center
21000 Brookpark Road
Cleveland, Ohio 44135

Library
NASA Lewis Research Center
21000 Brookpark Road
Cleveland, Ohio 44135 (2)

Report Control Office
NASA Lewis Research Center
21000 Brookpark Road
Cleveland, Ohio 44135

Brooklyn Polytechnic Institute
Attn: V. D. Agosta
Long Island Graduate Center
Route 110
Farmingdale, New York 11735

Chemical Propulsion Information Agency
Johns Hopkins University/APL
Attn: T. W. Christian
8621 Georgia Avenue
Silver Spring, Maryland 20910

NASA
Lewis Research Center
Attn: E. W. Conrad, MS 500-204
21000 Brookpark Road
Cleveland, Ohio 44135

North American Rockwell Corporation
Rocketdyne Division
Attn: L. P. Combs, D/991-350, Zone 11
6633 Canoga Park, California 91304

National Technical Information Service
Springfield, Virginia 22151
(40 Copies)

Aerospace Corporation
Attn: O. W. Dykema
Post Office Box 95085
Los Angeles, California 90045

Ohio State University
Department of Aeronautical and Astronautical Engineering
Attn: R. Edse
Columbus, Ohio 43210

TRW Systems
Attn: G. W. Elverum
One Space Park
Redondo Beach, California 90278

Bell Aerospace Company
Attn: T. F. Ferger
Post Office Box 1
Mail Zone J-81
Buffalo, New York 14205

Pratt & Whitney Aircraft
Florida Research & Development Center
Attn: G. D. Garrison
Post Office Box 710
West Palm Beach, Florida 33402

NASA
Lewis Research Center
Attn: L. Gordon, MS 500-209
21000 Brookpark Road
Cleveland, Ohio 44135

Purdue University
School of Mechanical Engineering
Attn: R. Goulard
Lafayette, Indiana 47907

Air Force Office of Scientific Research
Chief Propulsion Division
Attn: Lt. Col. R. W. Haffner (NAE)
1400 Wilson Boulevard
Arlington, Virginia 22209

NASA Representative
NASA Scientific and Technical
Information Facility
P. O. Box 33
College Park, Maryland 20740
(2 Copies with Document Release
Authorization Form)

University of Illinois
Aeronautics/Astronautic Engineering
Department
Attn: R. A. Strehlow
Transportation Building, Room 101
Urbana, Illinois 61801

NASA
Manned Spacecraft Center
Attn: J. G. Thibadaux
Houston, Texas 77058

Massachusetts Institute of Technology
Department of Mechanical Engineering
Attn: T. Y. Toong
77 Massachusetts Avenue
Cambridge, Massachusetts 02139

Illinois Institute of Technology
Attn: T. P. Torda
Room 200 M. H.
3300 S. Federal Street
Chicago, Illinois 60616

AFRPL
Attn: R. R. Weiss
Edwards, California 93523

U. S. Army Missile Command
AMSMI-RKL, Attn: W. W. Wharton
Redstone Arsenal, Alabama 35808

University of California
Aerospace Engineering Department
Attn: F. A. Williams
Post Office Box 109
LaJolla, California 92037

Georgia Institute of Technology
School of Aerospace Engineering
Attn: B. T. Zinn
Atlanta, Georgia 30332

Pennsylvania State University
Mechanical Engineering Department
Attn: G. M. Faeth
207 Mechanical Engineering Bldg.
University Park, Pennsylvania 16802

TISIA
Defense Documentation Center
Cameron Station
Building 5
5010 Duke Street
Alexandria, Virginia 22314

Office of Assistant Director
(Chemical Technician)
Office of the Director of Defense
Research and Engineering
Washington, D. C. 20301

D. E. Mock
Advanced Research Projects Agency
Washington, D. C. 20525

Dr. H. K. Doetsch
Arnold Engineering Development Center
Air Force Systems Command
Tullahoma, Tennessee 37389

Library
Air Force Rocket Propulsion
Laboratory (RPR)
Edwards, California 93523

Library
Bureau of Naval Weapons
Department of the Navy
Washington, D. C.

Library
Director (Code 6180)
U. S. Naval Research Laboratory
Washington, D. C. 20390

APRP (Library)
Air Force Aero Propulsion Laboratory
Research and Technology Division
Air Force Systems Command
United States Air Force
Wright-Patterson AFB, Ohio 45433

Marshall Industries
Dynamic Science Division
2400 Michelson Drive
Irvine, California 92664

Mr. Donald H. Dahlene
U. S. Army Missile Command
Research, Development, Engineering
and Missile Systems Laboratory
Attn: AMSMI-RK
Redstone Arsenal, Alabama 35809

Library
Bell Aerosystems, Inc.
Box 1
Buffalo, New York 14205

Report Library, Room 6A
Battelle Memorial Institute
505 King Avenue
Columbus, Ohio 43201

D. Suichu
General Electric Company
Flight Propulsion Laboratory
Department
Cincinnati, Ohio 45215

Library
Ling-Temco-Vought Corporation
Post Office Box 5907
Dallas, Texas 75222

Marquardt Corporation
16555 Saticoy Street
Box 2013 - South Annex
Van Nuys, California 91409

P. F. Winternitz
New York University
University Heights
New York, New York

R. Stiff
Propulsion Division
Aerojet-General Corporation
Post Office Box 15847
Sacramento, California 95803

Technical Information Department
Aeronutronic Division of Philco
Ford Corporation
Ford Road
Newport Beach, California 92663

Library-Documents
Aerospace Corporation
2400 E. El Segundo Boulevard
Los Angeles, California 90045

Library
Susquehanna Corporation
Atlantic Research Division
Shirley Highway and Edsall Road
Alexandria, Virginia 22314

STL Tech. Lib. Doc. Acquisitions
TRW System Group
One Space Park
Redondo Beach, California 90278

Dr. David Altman
United Aircraft Corporation
United Technology Center
Post Office Box 358
Sunnyvale, California 94088

Library
United Aircraft Corporation
Pratt & Whitney Division
Florida Research and Development
Center
Post Office Box 2691
West Palm Beach, Florida 33402

Library
Air Force Rocket Propulsion
Laboratory (RPM)
Edwards, California 93523

Allan Hribar, Assistant Professor
Post Office Box 5014
Tennessee Technological University
Cookeville, Tennessee 38501

NASA
Lewis Research Center
Attn: E. O. Bourke, MS 500-209
21000 Brookpark Road
Cleveland, Ohio 44135

Library, Department 596-306
Rocketdyne Division of Rockwell
North American Rockwell, Inc.
6633 Canoga Avenue
Canoga Park, California 91304

Library
Stanford Research Institute
333 Ravenswood Avenue
Menlo Park, California 94025

Rudy Reichel
Aerophysics Research Corp.
Post Office Box 187
Bellevue, Washington 98009

Princeton University
James Forrestal Campus Library
Attn: D. Harrje
Post Office Box 710
Princeton, New Jersey 08540

U. S. Naval Weapons Center
Attn: T. Inouye, Code 4581
China Lake, California 93555

Office of Naval Research
Navy Department
Attn: R. D. Jackel, 473
Washington, D. C. 20360

Air Force Aero Propulsion Laboratory
Attn: APTC Lt. M. Johnson
Wright-Patterson AFB, Ohio 45433

Naval Underwater Systems Center
Energy Conversion Department
Attn: Dr. R. S. Lazar, Code TB 131
Newport, Rhode Island 02840

NASA
Langley Research Center
Attn: R. S. Levine, MS 213
Hampton, Virginia 23365

Aerojet General Corporation
Attn: David A. Fairchild, Mech. Design
Post Office Box 15847 (Sect. 9732)
Sacramento, California 95809

NASA
Lewis Research Center, MS 500-313
Rockets & Spacecraft Procurement Section
21000 Brookpark Road
Cleveland, Ohio 44135

NASA
Lewis Research Center
Attn: H. W. Douglass, MS 500-205
21000 Brookpark Road
Cleveland, Ohio 44135

University of Michigan
Aerospace Engineering
Attn: J. A. Nicholls
Ann Arbor, Michigan 48104

Tulane University
Attn: J. C. O'Hara
6823 St. Charles Avenue
New Orleans, Louisiana 70118

University of California
Department of Chemical Engineering
Attn: A. K. Oppenheim
6161 Etcheverry Hall
Berkeley, California 94720

Army Ballistics Laboratories
Attn: J. R. Osborn
Aberdeen Proving Ground, Maryland 21005

Sacramento State College
School of Engineering
Attn: F. H. Reardon
6000 J. Street
Sacramento, California 95819

Purdue University
School of Mechanical Engineering
Attn: B. A. Reese
Lafayette, Indiana 47907

NASA
George C. Marshall Space Flight Center
Attn: R. J. Richmond, SNE-ASTN-PP
Huntsville, Alabama 35812

Colorado State University
Mechanical Engineering Department
Attn: C. E. Mitchell
Fort Collins, Colorado 80521

University of Wisconsin
Mechanical Engineering Department
Attn: P. S. Myers
1513 University Avenue
Madison, Wisconsin 53706

North American Rockwell Corporation
Rocketdyne Division
Attn: J. A. Nestlerode,
AC46 D/596-121
6633 Canoga Avenue
Canoga Park, California 91304

Jet Propulsion Laboratory
California Institute of Technology
Attn: J. H. Rupe
4800 Oak Grove Drive
Pasadena, California 91103

University of California
Mechanical Engineering Thermal Systems
Attn: Professor R. Sawyer
Berkeley, California 94720

ARL (ARC)
Attn: K. Scheller
Wright-Patterson AFB, Ohio 45433